DISPERSION IN ANISOTROPIC POROUS MEDIA

THESIS FOR THE DEGREE OF PH.D.
MICHIGAN STATE UNIVERSITY

JOHN RODGER ADAMS
1966

V. E. Custis

Major professor

Date Nov 28, 1966

O-169

A B S T R A C T

DISPERSION IN ANISOTROPIC POROUS MEDIA

by

John Rodger Adams

The problem of dispersion in flow through porous media arises in coastal aquifers, underground waste disposal, chemical separation by filtration, and secondary recovery of petroleum. This study is motivated by the coastal aquifer problem in which the spread or dispersion of salt water into fresh water may limit the use of wells for drinking water. The dispersion process is described by the convective-diffusion equation with a coefficient depending on the flow and porous medium as well as on the solvent and solute. The nature and functional form of the coefficient is the topic of direct interest.

Existing theories state that the dispersion coefficient is a second rank tensor formed by the contraction of a fourth rank tensor dependent on the porous medium with a second rank tensor dependent on the flow. This theory, which is presented for isotropic media, is adapted to anisotropic media by a transformation of coordinates involving the permeability tensor. Experiments are conducted in which the dispersion of tracer spots is measured during flow in porous beds packed with nylon filaments. The filaments are kept parallel to make the bed anisotropic . Two filament sizes and two orientations are used.

The experimental results are in reasonable agreement with previous experiments in isotropic media but are not compatible with the existing theory. A new relation is proposed in which the tensor dispersion coefficient is equal to the contraction of a second rank tensor depending on the fluid and solid media with a second rank tensor depending on the flow. The power to which the velocity appears in the flow-dependent tensor is expected to depend on the: (1) angle between the flow and major permeability, (2) flow channel geometry, (3) the component.

DISPERSION IN ANISOTROPIC POROUS MEDIA

by

John Rodger Adams

A THESIS

Submitted to
Michigan State University
in partial fulfillment of the requirements
for the degree of

DOCTOR OF PHILOSOPHY

Department of Civil Engineering

1966

ACKNOWLEDGMENTS

The author wishes to express his gratitude to Dr. H. R. Henry who suggested the topic and provided the inspiration to undertake the work. The support, encouragement, and patience of Dr. C. E. Cutts, Chairman of the Department of Civil and Sanitary Engineering, who urged the author along during trying times, is greatly appreciated. The author wishes to thank the committee members for their constructive criticism. Especial thanks are due to Dr. J. S. Frame, Professor, Department of Mathematics, for his careful explanations. Financial support from the Institute of Water Research, Dr. L. L. Quill, Director; and the Division of Engineering Research, Mr. J. W. Hoffman, Director, is acknowledged.

TABLE OF CONTENTS

	Page
ACKNOWLEDGMENTS	ii
LIST OF TABLES	v
LIST OF FIGURES	vi
LIST OF SYMBOLS	viii
1. INTRODUCTION	1
2. THEORY	
2.1 General	5
2.2 Flow through Anisotropic Porous Media	6
2.3 Dispersion	15
3. EXPERIMENTAL APPARATUS AND PROCEDURE	
3.1 Apparatus	26
3.2 Procedure	29
3.3 Discussion of Procedure	31
3.4 Discussion of Experiments	33
4. DATA ANALYSIS	
4.1 Data Reduction	35
4.2 Presentation of Results	39
4.3 Discussion of Results	42
5. CONCLUSIONS	49

TABLE OF CONTENTS (continued)

	Page
APPENDIX	53
TABLES	56
FIGURES	69
BIBLIOGRAPHY	86

LIST OF TABLES

Table		Page
4-1	Parameters in Least Square Analysis of Tracer Distribution	56
4-2	Summary of Experimental Work	57
4-3	Data for Bed 1	58
4-4	Data for Bed 2	59
4-5	Data for Bed 3	60
4-6	Data for Bed 4	61
4-7	Equations of Lines Fit to data by Least Squares Method	62
4-8	Anisotropic Permeabilities	63
4-9	Transformed Dispersion Coefficients	64
A-1	Summary of Least Squares Check Computation Bed 1	65
A-2	Summary of Least Squares Check Computation Bed 2	66
A-3	Summary of Least Squares Check Computation Bed 3	67
A-4	Summary of Least Squares Check Computation Bed 4	68

LIST OF FIGURES

Figure		Page
2-1	Flow Region in Anisotropic Medium	12
2-2	Transformed Flow Region-Isotropic Medium	13
3-1	Schematic Drawing of Apparatus	69
3-2	Overall View of Apparatus	70
3-3	Porous Bed and Electrode Group	70
3-4	Inlet Constant Head Tank	71
3-5	Outlet Constant Head Tank	71
3-6	Electrode Groups	72
4-1	Concentration of NaCl in water as a function of Specific Conductance	73
4-2	Molecular Diffusivity and Kinematic Viscosity	74
4-3a	Bed 1 Dx/Dm versus Pe	75
4-3b	Bed 1 Dy/Dm versus Pe	76
4-4a	Bed 2 Dx/Dm versus Pe	77
4-4b	Bed 2 Dy/Dm versus Pe	78
4-5a	Bed 3 Dx/Dm versus Pe	79
4-5b	Bed 3 Dy/Dm versus Pe	80
4-6a	Bed 4 Dx/Dm versus Pe	81
4-6b	Bed 4 Dy/Dm versus Pe	82
4-7	Composite Plot of Data	83
A-1	Bed 1 R/R_{LS} versus n/n_{LS}	84

LIST OF FIGURES (continued)

Figure		Page
A-2	Bed 3 R/R_{LS} versus n/n_{LS}	84
A-3	Bed 2 R/R_{LS} versus n/n_{LS}	85
A-4	Bed 4 R/R_{LS} versus n/n_{LS}	85

LIST OF SYMBOLS

Common symbols are listed here. Symbols which appear rarely are defined in the text.

Symbol	Description	Dimensions
A	Area	L^2
A^{ij}_{kl}	Media dispersivity tensor, isotropic media	L^2/T
a^{ij}_{kl}	Media dispersivity tensor, anisotropic media	L^2/T
B	Cell constant	$1/L$
B'	Cell constant for electrode	$1/L$
c	Concentration	M/L^3
d	Diameter of solid medium element	L
D^{ij}	Dispersion coefficient tensor, isotropic media	L^2/T
d^{ij}	Dispersion coefficient tensor, anisotropic media	L^2/T
D_m	Molecular diffusion constant	L^2/T
F^{kl}	Flow dispersion factor tensor, isotropic media	
f^{kl}	Flow dispersion factor tensor, anisotropic media	
g	Acceleration of gravity	L/T^2
g^{ij}	Metric tensor	
h	Head	L
I, II	Subscripts indicating major and minor principal values of symmetric second order tensors	
k^{ij}	Permeability tensor	L^2

LIST OF SYMBOLS (continued)

Symbol	Description	Dimensions
K_r	Permeability ratio, k_I/k_{II}	
P	Porosity	
p	Pressure	M/LT^2
Pe	Peclet number, ud/D_m	
Re	Reynolds number, ud/ν	
$1/R$	Measured conductivity	micromhos
$1/R_o$	Measured conductivity of base fluid	micromhos
$1/R'$	Electrode conductivity of base fluid	micromhos
T	Temperature	^oC
t	Time	T
u^i	Velocity component	L/T
V	Volume	L^3
X^i	Coordinates in isotropic medium	L
x^i	Coordinates in anisotropic medium	L
z	Vertical distance	L
α,β	Angles between flow direction and k_I direction	
γ	Unit weight	M/L^2T^2
Δ	Increment or difference	
ξ,η	Coordinates parallel and perpendicular to flow	L
μ	Viscosity	M/LT
ρ	Mass density	M/L^3
$1/\rho$	Specific conductance	micromhos/L
$1/\rho_o$	Specific conductance of base fluid	micromhos/L

LIST OF SYMBOLS (continued)

Symbol	Description	Dimensions
$1/\rho_c$	Specific conductance of solution (salt only)	micromhos/L
σ	Standard deviation	L

1. INTRODUCTION

The problem of the dispersion or spread of a fluid or solution imbedded in another fluid flowing through a porous medium has been of interest to engineers for many years. One of the early problems which has taken on even greater importance is the fresh water-salt water interaction in groundwater aquifers along sea coasts. Knowledge of the location and mobility of the interface (or mixing zone) is critical to the location and operation of wells supplying water for domestic use in coastal regions. A problem of more recent concern is the contamination of groundwater sources by industrial or municipal wastes. These wastes may enter aquifers either by infiltration or through the use of subsurface formations for the disposal of concentrated or hard to treat liquid wastes. Chemical and petroleum engineers also have definite interests in dispersion during the flow through porous media. Chemicals may be separated by use of the different dispersion of each material during the flow through filter columns. The success of secondary recovery of oil by water or hydrocarbon displacement depends on the ability to avoid excessive mixing.

The initial efforts at analysis of the fresh-salt water interface assumed that both fluids were static and that they were immiscible. These assumptions lead to the well known Gyben-Herzberg

relation between water table and interface elevations, (Todd, 1959)[1]. The next degree of approximation is to consider flow in the fresh water only and to retain the immiscible assumption. Henry (1959) obtained solutions for fresh water outflow through a vertical surface by means of the hodograph and complex mapping. De Josselin de Jong (1959) avoided the difficulty imposed by the need for two potential functions when motion is allowed in the salt water by representing the sharp interface by a distribution of vortices. As a follow-up to Henry's work, Lin (1964) used singularities to describe the interfacial discontinuities and used numerical integration to obtain a solution for the movement of the interface after a sudden change in fresh water flow rate.

Somewhat parallel to the studies above, the effect of miscibility was included in efforts to describe the actual mixing zone between fresh and salt water. Wentworth (1948) and Carrier (1958) showed that molecular diffusion was unimportant compared with the macroscopic dispersion in the development of transition zones. Henry (1960) solved the problem including dispersion by an approximate method and obtained streamlines and isochlors which agree with field data (Kohout, 1960).

The success of these calculations of the mixing region obviously depends on the accuracy of the description of the dispersion process. The simplest approach is to use a scalar dispersion coefficient. However, reference to Ogata and Banks (1961) and Ogata (1961) shows that the dispersion in the flow direction is several times the dispersion in the transverse direction. One approach is exemplified by

[1]Dates in parentheses refer to references in the bibliography.

von Rosenberg's (1956) combination of the capillary model of porous medium (Scheidegger, 1960) and Taylor's (1953) theory of dispersion in circular tubes. Another approach is the use of statistics to describe the porous medium or the flow pattern. Scheidegger (1954) considered the dispersive nature of the flow of a single fluid through a porous medium. De Jong (1958) and Saffman (1959) applied stochastic processes in order to obtain dispersion coefficients. Saffman and De Jong arrived at similar results for longitudinal dispersion including the influence of molecular diffusion, but while De Jong predicted a ratio of lateral to longitudinal dispersion dependent on the distance traveled, Saffman predicted that lateral dispersion was entirely independent of molecular diffusion. This last statement is in opposition to that of Simpson (1962) who states that molecular diffusion is the primary mechanism of lateral dispersion. In a second paper (1960), Saffman obtains values of dispersion coefficients which are valid for all values of the Peclet number.

Still another view of the dependence of the dispersion coefficient on the fluid, the porous medium, and the macroscopic flow pattern has been developed recently. Papers by Bear (1961) and Scheidegger (1961) propose that the dispersion coefficient is a symmetric second order tensor formed by the contraction of a fourth order tensor which depends on the porous medium and a second order tensor which is a function of the flow. Harleman and Rumer (1962) suggest that the manner of dependence on the flow is non-linear with the power of the velocity variable from component to component.

The merit of the last approach will be studied experimentally. The ultimate success would be to determine the relations for the tensor dispersion coefficient and flow function. However, the experimental results raise severe doubts about the validity of this theory. Conventionally plotted results lead to expressions which are not compatible with the theoretical requirements. A possible extension of the original theory is proposed as is an alternative theory involving a second rank tensor for the media factor. The theoretical development will not include a solution of the convective dispersion equation but will attempt to present the dispersion process in anisotropic porous media in terms of the measured quantities. The anisotropic media is vital to the study as it should aid in exposing the effect of the solid medium, which is considered to be more significant than the fluid part of the system.

2. THEORY

2.1 General

The theory of flow through porous media, including the transformation between anisotropic media and isotropic media, will be treated first. The flow will be assumed to be slow, and laminar so that Darcy's law will apply. The transformation is used to replace an anisotropic medium in which the flow is not described by the Laplace equation with an isotropic medium in which the flow is described by the Laplace equation, but the domain is distorted. After this, the dispersion equation will be treated. The transformation will be used to aid in understanding the dispersion process in anisotropic media by applying it to what is known about dispersion in isotropic media. The treatment will center around the tensor dispersion coefficient and will essentially assume that the region is infinite in extent.

As the nature of the transformation is not proper to Cartesian tensors[1], general tensor notation must be used in that part of the development. For continuity, general tensor notation will be used throughout. The operations concerning tensors generally follow the book by Aris (1962). A vector may be represented by its contravariant components which transform according to:

$$\bar{a}^i = \frac{\partial \bar{x}^i}{\partial x^j} a^j \qquad (1)$$

[1] Aris (1962) states that "The group of rotations ... is the only group of transformations considered in constructing Cartesian tensors."

A vector may also be represented by its covariant components which transform according to:

$$\bar{a}_i = \frac{\partial x^j}{\partial \bar{x}^i} a^j \qquad (2)$$

Summation is implied by the appearance of the same index as both an upper and lower suffix in the same term. Note that an upper index in the denominator counts as a lower index in the equation. If an index appears only once in each term, it may assume any value in the range of the indices. Where details are required, the treatment will be two dimensional to save space and to prepare for the two dimensional experimental work. Thus the indices range over the values 1 and 2.

2.2 Flow through anisotropic porous media

The flow of an incompressible fluid can be described by two differential equations and appropriate boundary conditions. The conservation of mass is given by the incompressible continuity equation as:

$$\frac{\partial u^i}{\partial x^i} = 0 \qquad (3)$$

where: u^i = velocity in the x^i direction

The equation of motion is the Navier-Stokes equation, which is given by Aris (1962) as:

$$\rho \frac{Du^i}{Dt} = - g^{ij} \left(\gamma \frac{\partial z}{\partial x^j} + \frac{\partial p}{\partial x^j}\right) + \mu g^{jk} \frac{\partial^2 u^i}{\partial x^j \partial x^k} \qquad (4)$$

where: z is measured vertically upward

p = pressure

ρ = mass density

γ = unit weight

μ = viscosity

g^{ij} = metric tensor

$$\frac{D}{Dt} = \frac{\partial}{\partial t} + u^j \frac{\partial}{\partial x^i}$$

This equation (4) is valid for an incompressible fluid in a gravitational field. Note that for Cartesian coordinates $g^{ij} = 0$ if $i = j$, and $g^{ii} = 1$. For steady motion the first term in the acceleration is zero. For sufficiently slow motion the remaining terms in the acceleration are small, so that, for slow steady flow Eq. 4 may be written as:

$$g^{ij} \left(\gamma \frac{\partial z}{\partial x^j} + \frac{\partial p}{\partial x^j}\right) = \mu \, g^{jk} \frac{\partial^2 u^i}{\partial x^j \partial x^k} \tag{5}$$

It is convenient to replace the lefthand side of Eq. 5 by $\gamma \frac{\partial h}{\partial x^i}$, with $h = p/\gamma + z$, so that the equation of motion becomes:

$$\frac{\partial h}{\partial x^i} = \frac{\mu}{\gamma} g^{jk} \frac{\partial^2 u^i}{\partial x^j \partial x^k} \tag{6}$$

However, this equation applies to each particle of fluid flowing through the flow channels between the solid particles. The complex and unknown geometry of the pore spaces precludes the formulation of the boundary value problem, let alone the solution of it. Darcy's law for the bulk velocities is used in porous media problems and will be used here. A generalized form of Darcy's law (Collins, 1961) is:

$$u^i = - \frac{\gamma}{P\mu} k^{ij} \frac{\partial h}{\partial x^j} \tag{7}$$

where: P = porosity

k^{ij} = permeability tensor

This equation (7) is valid for a homogeneous medium, in which the permeability is not a function of location. Note that the velocity vector and the head gradient are not necessarily parallel.

The relation between Eqs. 6 and 7 must be made very clear. The velocity in Eq. 6 is a point function defined in the region consisting of the pore space in the porous medium. The velocity in Eq. 7 is an artificial average velocity equal to the volume flow rate divided by the area of the pore space in the appropriate direction. The same sort of thing is true of the head gradients. The head gradient in Eq. 6 is evaluated at a point in the actual flow while the head gradient in Eq. 7 is again an average over a portion of the bed. Thus the Navier-Stokes equation and the complex geometry are replaced by the Darcy equation and an homogeneous continuum.

The complete derivation of Darcy's law from the Navier-Stokes equation is practically impossible. Any geometric model of a porous medium which would permit solution of the Navier-Stokes equations would be too regular to be a good model of a real porous medium. However, the concept of the "capillary bundle" theory (Collins, 1961) can help one to understand the interrelation. The porous medium is considered to be a collection of parallel tubes of various cross sections. The solution of the Navier-Stokes equation for steady flow

through a straight tube of uniform cross section yields the following expression for the average velocity in the tube:

$$v^1 = -\frac{S}{\mu}\frac{\partial h}{\partial x^1} \tag{8}$$

where: the tube axis is in the x^1 direction

S is the constant dependent on the shape of the cross section

v^1 is the average velocity in the tube

There is a strong similarity in form between Eq. 8 and Eq. 7. There are still the undetermined relations between the velocities and between the head gradients in the two equations, as well as the effect of geometry on S and k^{ij}. The similarity is significant however, for if the geometric difficulties could be resolved, or if Eq. 6 could be solved for irregular geometries the derivation could be completed. Such efforts are not of interest in this project.

For the purpose at hand the flow of an incompressible fluid through a porous medium will be described by Eq. 3, Eq. 7 and the appropriate boundary conditions, which are:

1) h = constant (or function of time) on boundaries open to a reservoir

2) $u^h = 0$ on impermeable boundaries

where: u^n is the velocity component normal to the boundary.

If Eq. 7 is substituted into Eq. 3 the following equation is obtained:

$$\frac{\partial}{\partial x^i}\left\langle (-k^{ij}\frac{\gamma}{\mu}\frac{\partial h}{\partial x^j})\right\rangle = 0 \qquad (9)$$

Since the medium has been assumed to be homogeneous this may be written:

$$k^{ij}\frac{\partial^2 h}{\partial x^i \partial x^j} = 0 \qquad (9a)$$

Furthermore, if the medium is isotropic, Laplace's equation is obtained:

$$\frac{\partial^2 h}{\partial x^1 \partial x^1} + \frac{\partial^2 h}{\partial x^2 \partial x^2} = 0 \qquad (10)$$

Standard mathematical techniques yield solution to flow problems in most cases if the medium is isotropic. Collections of solutions to Laplace's equation with reference to groundwater problems can be found in several books, including those by Harr (1962), Muskat (1946), and Polubarinova-Kochina (1962).

The solution of Eq. 9, however, is more difficult But a change of variable involving a scale change will convert the anisotropic medium into an isotropic one. Though several variations are possible, the transformation used here will be a scale change in the direction of the minor permeability. The transformation is carried out after the flow region in the anisotropic medium has been expressed in the coordinate system which coincides with the principal axes of the permeability tensor. The existence of these axes depends on the assumption that the permeability tensor is symmetric. The relation between the coordinates

convenient for the flow region and the principal axes of the permeability are given by the rotation:

$$\begin{pmatrix} \xi \\ \eta \end{pmatrix} = \begin{pmatrix} \cos\alpha & \sin\alpha \\ -\sin\alpha & \cos\alpha \end{pmatrix} \begin{pmatrix} x \\ y \end{pmatrix} \tag{11}$$

The angle is determined by the relation:

$$\begin{pmatrix} k^{11} & k^{12} \\ k^{21} & k^{22} \end{pmatrix} = \begin{pmatrix} \cos\alpha & -\sin\alpha \\ \sin\alpha & \cos\alpha \end{pmatrix} \begin{pmatrix} k_I & 0 \\ 0 & k_{II} \end{pmatrix} \begin{pmatrix} \cos\alpha & \sin\alpha \\ -\sin\alpha & \cos\alpha \end{pmatrix} \tag{12}$$

where k_I and k_{II} are the major and minor principal values of the permeability.

In the x, y coordinate system, Eq. 9a becomes:

$$k_I \frac{\partial^2 h}{\partial x^2} + k_{II} \frac{\partial^2 h}{\partial y^2} = 0 \tag{13}$$

Now let $K_r = k_I/k_{II}$, $X = x$, and $Y = y/K_r$ in Eq. 13:

$$k_I \frac{\partial^2 h}{\partial X^2} + k_{II} K_r \frac{\partial^2 h}{\partial Y^2} = 0 \tag{14}$$

This is of course Laplace's equation. The medium in the X, Y plane is isotropic with permeability k_I.

Now consider the transformation in some detail by applying it to a rectangular region in the ξ, η plane, with the permeability directions as shown in Fig. 2-1. The η axis is vertical. The components of the permeability tensor in the ξ, η plane are given by Eq. 12. The boundary conditions are: $h = 0$, $\xi = L$; $h = h_o$, $\xi = 0$; $\frac{\partial h}{\partial \eta} = 0$, $\eta = 0$, and $\eta = H$.

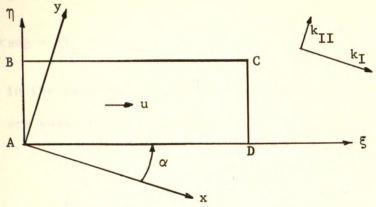

Fig. 2-1 Flow Region in Anisotropic Medium

The transformation to the isotropic medium is now:

$$X = x = \xi \cos\alpha - \eta \sin\alpha$$
$$Y = y\sqrt{k_r} = \sqrt{k_r}\,(\xi \sin\alpha + \eta \cos\alpha) \tag{15}$$

A further rotation into a ξ', η' system, in which ξ' is parallel to the long side of the region may be defined by the appropriate substitutions into Eq. 11. An angle β may be found in terms of the angle α and the permeability ratio as follows. The ξ' axis is given by the equation:

$$-X \sin\beta + Y \cos\beta = 0$$
or $$Y = X \tan\beta \tag{16}$$

But in the anisotropic medium the ξ axis is given by the equation:

$$-x \sin\alpha + y \cos\alpha = 0$$
or $$y = x \tan\alpha \tag{17}$$

Now by use of Eq. 15 in Eq. 17

$$Y = \sqrt{k_r}\, X \tan\alpha \tag{18}$$

And equating Eqs. 18 and 16 it is found that:

$$\tan\beta = \sqrt{k_r}\,\tan\alpha \tag{19}$$

The region in the isotropic medium is shown in Fig. 2-2. The boundary conditions are essentially unchanged.

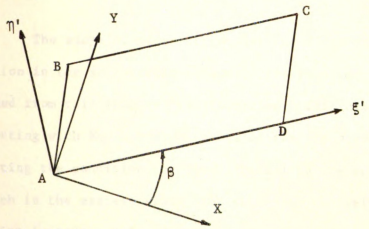

Fig. 2-2 Transformed Flow Region -- Isotropic Medium

In this plane there must be end regions of curvilinear flow. In the center of the region the long boundaries will force the velocity to be parallel to the ξ' direction. However, the velocity will be perpendicular to the permeable ends which are also lines of constant head. This follows immediately from the fact that the solutions of Laplace's equation in terms of stream function or a potential function are orthogonal. This streamline curvature will remain after transforming back into the rectangular domain in the anisotropic medium. Curvilinear flow will affect the dispersion and this is an unnecessary complication. If the medium were sufficiently long it would be possible to use the central section only for the dispersion tests. This would probably require excessively long apparatus since the ends can be

expected to influence the flow pattern within the bed to a distance the same size as the height of the end. The transformation itself suggests another way to avoid this trouble. A rectangular region in the isotropic medium would have parallel flow throughout, and this could be transformed into a parallelogram shaped region in the anisotropic region, also with parallel flow.

The slope of lines of constant head for flow in a given direction in the anisotropic medium is the important thing to be obtained from this inverse transformation. This slope can be obtained by starting with Eq. 9, by making use of the transformation, or by inspecting the condition for flow parallel to the axis. The last approach is the easiest since, for this flow the velocity in the η direction is zero and Eq. 7 yields:

$$u^1 = -\frac{\gamma}{P\mu}\left(k^{11}\frac{\partial h}{\partial \xi} + k^{12}\frac{\partial h}{\partial \eta}\right)$$
$$u^2 = -\frac{\gamma}{P\mu}\left(k^{21}\frac{\partial h}{\partial \xi} + k^{22}\frac{\partial h}{\partial \eta}\right) \qquad (20)$$

These equations may be solved to yield:

$$\frac{\partial h}{\partial \xi} = -\frac{u^1 k^{22}}{k^{11}k^{22} - k^{12}k^{21}}$$
$$\frac{\partial h}{\partial \eta} = \frac{u^1 k^{21}}{k^{11}k^{22} - k^{12}k^{21}} \qquad (21)$$

Now along lines of constant head, the total differential of the head is zero, or:

$$0 = \frac{\partial h}{\partial x}\,dx + \frac{\partial h}{\partial y}\,dy \qquad (22)$$

This may be solved for:

$$\frac{d\eta}{d\xi} = \frac{\frac{\partial h}{\partial \xi}}{\frac{\partial h}{\partial \eta}} \tag{23}$$

Now substituting from Eqs. 20 and 13 the slope of the lines of constant head becomes:

$$\frac{\partial \eta}{\partial \xi} = \frac{\cos^2\alpha + K_r \sin^2\alpha}{(K_r - 1)\sin\alpha \cos\alpha} \tag{24}$$

The apparent difficulty which is caused by $\alpha = 0$, $\alpha = \pi/2$, or $k_I = k_{II}$, for which values the denominator of Eq. 21 becomes zero, may be resolved in each case by returning to the original statement of the problem. In each of these cases $k^{12} = k^{21} = 0$ so the rotation to principal axes is not necessary, and the velocity vector is perpendicular to the lines of constant head.

2.3 Dispersion

A brief dimensional discussion is of interest before proceeding with the treatment of the dispersion coefficient. The convective-diffusion equation which is a mass conservation statement for the tracer is (Bear, 1961):

$$\frac{\partial c}{\partial t} + u^i \frac{\partial c}{\partial x^i} - \frac{\partial}{\partial x^i}\left(D^{ij} \frac{\partial c}{\partial x^j}\right) = 0 \tag{25}$$

where: c = tracer concentration

t = time

D^{ij} = dispersion coefficient

This is valid for a substance of concentration c embedded in an incompressible fluid (Henry, 1960).

Though a dimensionlal analysis of the combined problem of flow with dispersion does not result in a useful basis for analysis, some discussion of the dimensional nature of the dispersion coefficient is helpful. The convective-diffusion equation may be put into dimensionless form by the following substitution:

$$\bar{x}^i = x^i/d$$

$$\bar{c} = c/c_o$$

$$\bar{u}^i = u^i/u_o$$

$$\bar{D}^{ij} = D^{ij}/D_m$$

$$\bar{t} = tu_o/d$$

where: The overscored quantities are dimensionless, d is diameter of solid material and D_m is the effective molecular diffusivity.

If this substitution is made into a one-dimensional form of the convective-diffusion equation the following expression results:

$$\frac{u_o c_o}{d}\frac{\partial \bar{c}}{\partial \bar{t}} + \frac{u_o c_o}{d}\bar{u}^1\frac{\partial \bar{c}}{\partial \bar{x}^1} = \frac{D_m c_o}{d^2}\bar{D}^{11}\frac{\partial^2 \bar{c}}{\partial \bar{x}^1 \partial \bar{x}^1} \qquad (26)$$

Now divide by $u_o c_o/d$ to obtain

$$\frac{\partial \bar{c}}{\partial \bar{t}} + \bar{u}^1\frac{\partial \bar{c}}{\partial \bar{x}^1} = \frac{D_m}{u_o d}\bar{D}^{11}\frac{\partial^2 \bar{c}}{\partial \bar{x}^1 \partial \bar{x}^1} \qquad (26a)$$

The parameter $D_m/u_o d$ is the reciprocal of the Peclet number and appears in the same manner as the reciprocal of the Reynolds number appears in the Navier-Stokes equation. For a fluid-tracer mixture in a porous medium the effective molecular diffusivity is a function of the porosity as well as the molecular diffusivity of the tracer in fluid. If there is no flow, molecular diffusion will take place but the rate is reduced by the interference of the solid medium. On the other hand, if even slow flow occurs, the porous material causes larger scale mixing and the dispersion is much more than could be caused by molecular diffusion alone. Of course the actual transfer of tracer material across streamlines is always due to molecular action in laminar flow. So long as the flow within the pore spaces remains laminar, the Reynolds number should not be used as the independent variable. Instead the ratio of D to D_m should be a function of the Peclet number.

Unfortunately, dimensional reasoning does not help much when an effort is made to determine the functional relation. Scheidegger (1961) and Bear (1961) propose that the dispersion coefficient is given by the contraction of a fourth order tensor dependent on the porous medium with a second order tensor dependent on the flow.

$$D^{ij} = A^{ij}_{kl} F^{kl} \tag{27}$$

This is only an hypothesis and the results of this study do not support it, at least when the usual analysis is carried out. The medium factor has dimensions of length and the flow factor has dimensions of velocity. But, as Harleman and Rumer (1962) point out, the experimental evidence

does not support the requirement that the velocity appear to the first power. In fact, they suggest that the exponent may vary from component to component. This requires that the dimensional nature of A^{ij}_{kl} and F^{kl} vary from element to element. In a later publication by Harleman, Mehlhorn, and Rumer (1963), all the dimensions are assigned to the medium factor and the flow factor is made dimensionless. This means that the medium factor depends on the fluid as well as the solid phase, since the time dimension can enter only with a fluid property such as the kinematic viscosity or the molecular diffusivity of the tracer. This in only indicated, not directly stated, in the 1963 paper by Harleman and associates.

Keeping equation 27 at hand, consider the properties of D^{ij} and A^{ij}_{kl} in isotropic media, and then use the transformation of the previous section to obtain some knowledge about their properties in the anisotropic media. However, since F^{kl} is expected to depend primarily on the velocity it is reasonable to expect that F^{kl} will have contravariant components. This agrees with the proposal of Scheidegger (1961), who assumed that $F^{kl} = j^k u^l / |u|$, which is symmetric. Scheidegger is concerned primarily with A^{ij}_{kl}, and by symmetry arguments similar to those used in crystal structure shows that for an isotropic medium there are only twenty-one non-zero elements in the three dimensional case. The number of non-zero elements in A^{ij}_{kl} reduces to eight (of sixteen) in two dimensions. He also shows that there are only two independent factors involved in the non-zero terms. Thus, in two dimensions:

$$A^{11}_{11} = A^{22}_{22} = A_I \tag{28}$$

$$A^{11}{}_{22} = A^{22}{}_{11} = A_{II}$$

$$A^{12}{}_{12} = A^{12}{}_{21} = A^{21}{}_{21} = (A_I - A_{II})/2 \qquad \text{(28 con't)}$$

and the other eight terms are zero.

In the isotropic medium the only preferred direction is the direction of flow. Therefore D^{ij} can be written as follows in the coordinate system pertinent to the domain and velocity:

$$\begin{aligned} D^{11} &= D_I \\ D^{22} &= D_{II} \\ D^{12} &= D^{21} = 0 \end{aligned} \qquad (29)$$

The contraction expressed in Eq. 26 is written out with $A^{ij}{}_{kl}$ given by Eq. 28, D^{ij} given by Eq. 29 and F^{kl} left undetermined.

$$\begin{aligned} D^{11} &= D_I = A_I F^{11} + A_{II} F^{22} \\ D^{12} &= 0 = \left((A_I - A_{II})/2 \right) (F^{12} + F^{21}) \\ D^{21} &= 0 = \left((A_I - A_{II})/2 \right) (F^{12} + F^{21}) \\ D^{22} &= D_{II} = A_{II} F^{11} + A_I F^{22} \end{aligned} \qquad (30)$$

The expressions for D^{12} and D^{21} imply that either $A_I = A_{II}$ or $F^{12} + F^{21} = 0$. But the experimental evidence that D_I and D_{II} and the relations for D^{11} and D^{22} require the second condition. A well known property of second rank tensors is that they may be written as the sum of a symmetric tensor and a skew-symmetric tensor. The

symmetry property is unchanged by a rotation. Also, the fourth rank tensor, $A^{ij}{}_{kl}$, is isotropic, and its components are not changed by a rotation. Thus a skew-symmetric portion of F^{kl} will never appear in D^{ij} and will be assumed to be zero for simplicity. Consequently, F^{kl} is also symmetric and may be written as:

$$F^{11} = F_I$$

$$F^{12} = F^{21} = 0 \tag{31}$$

$$F^{22} = F_{II}$$

Now Eq. 30 may be rewritten by substituting Eq. 31 for F^{kl}:

$$D^{11} = D_I = A_I F_I + A_{II} F_{II}$$

$$D^{12} = D^{21} = 0 \tag{32}$$

$$D^{22} = D_{II} = A_{II} F_I + A_I F_{II}$$

Though written in general tensor notation, equations 28 to 32 and the associated discussion apply to an isotropic porous medium. It is now possible to apply the transformation presented earlier in order to learn something about the dispersion coefficient in an anisotropic medium. It is necessary to keep very close tabs on the transformations because the inverse contravariant transformation is the same as the direct covariant transformation for this particular transformation.

It is convenient to write second order tensors as matrices, and it will be helpful to write out both contravariant and covariant, direct and inverse transformations.

Direct: from anisotropic to isotropic

Contravariant:
$$\begin{pmatrix} X \\ Y \end{pmatrix} = \begin{pmatrix} 1 & 0 \\ 0 & \sqrt{K_r} \end{pmatrix} \begin{pmatrix} x \\ y \end{pmatrix} \tag{33a}$$

Covariant:
$$\begin{pmatrix} X \\ Y \end{pmatrix} = \begin{pmatrix} 1 & 0 \\ 0 & \sqrt{\frac{1}{K_r}} \end{pmatrix} \begin{pmatrix} x \\ y \end{pmatrix} \tag{33b}$$

Inverse: from isotropic to anisotropic

$$\begin{pmatrix} x \\ y \end{pmatrix} = \begin{pmatrix} 1 & 0 \\ 0 & \sqrt{\frac{1}{K_r}} \end{pmatrix} \begin{pmatrix} X \\ Y \end{pmatrix} \tag{34a}$$

Covariant:
$$\begin{pmatrix} x \\ y \end{pmatrix} = \begin{pmatrix} 1 & 0 \\ 0 & \sqrt{K_r} \end{pmatrix} \begin{pmatrix} X \\ Y \end{pmatrix} \tag{34b}$$

These transformations may be applied to the three tensors given in Eqs. 28, 29, and 31. Eq. 12 indicates the appropriate form to carry out the transformation by matrix multiplication. The transformation may also be expressed by a contraction such as, $d^{ij} = T^{i}_{m} T^{j}_{n} D^{mn}$. The fourth rank tensor is best handled by writing out the contraction, since appropriate and conformable matrix representations would have to be figured out first. Now the dispersion coefficient in the anisotropic medium in terms of the dispersion coefficient in the isotropic medium is given by:

$$\begin{aligned} d^{11} &= D^{11} = D_I \\ d^{22} &= \frac{1}{K_r} \; D^{22} = \frac{1}{K_r} \; D_{II} \\ d^{12} &= d^{21} = 0 \end{aligned} \tag{35}$$

Similarly, the flow factor becomes:

$$f^{11} = F^{11} = F_I$$

$$f^{22} = \frac{1}{K_r} F^{22} = \frac{1}{K_r} F_{II} \tag{36}$$

$$f^{12} = f^{21} = 0$$

The fourth order tensor is best handled in several groups of components which transform similarly.

1) Components in which each index value occurs the same number of times as a lower suffix as it does as an upper suffix.

$$a^{11}{}_{11} = A^{11}{}_{11} = A_I$$

$$a^{22}{}_{22} = A^{22}{}_{22} = A_I$$

$$a^{12}{}_{12} = a^{12}{}_{21} = a^{21}{}_{12} = a^{21}{}_{21} = \tag{37a}$$

$$A^{12}{}_{12} = A^{12}{}_{21} = A^{21}{}_{12} = A^{21}{}_{21} = (A_I - A_{II})\ /2$$

2) Components in which both upper siffixes have the same value and both lower suffixes have the same value.

$$a^{11}{}_{22} = K_r\, a^{11}{}_{22} = K_r\, A_{II}$$

$$a^{22}{}_{11} = \frac{1}{K_r} A^{22}{}_{11} = \frac{1}{K_r} A_{II} \tag{37b}$$

3) Components in which one index value occurs only once.

$$a^{11}{}_{12} = \sqrt{K_r}\, A^{11}{}_{12} \qquad a^{11}{}_{21} = \sqrt{K_r}\, A^{11}{}_{21} \tag{37c}$$

$$a^{12}_{22} = \sqrt{K_r}\, A^{11}_{12} \qquad a^{21}_{22} = \sqrt{K_r}\, A^{21}_{22}$$

$$a^{22}_{12} = \frac{\sqrt{1}}{K_r} A^{22}_{12} \qquad a^{22}_{21} = \frac{\sqrt{1}}{K_r} A^{22}_{21} \qquad \text{(37c con't)}$$

$$a^{12}_{11} = \frac{\sqrt{1}}{K_r} A^{12}_{11} \qquad a^{21}_{11} = \frac{\sqrt{1}}{K_r} A^{21}_{11}$$

Since A^{ij}_{kl} is an isotropic tensor in the isotropic medium Eqs. 37 are valid regardless of the orientation of the flow and permeability. However, since D^{ij} and F^{kl} are aligned with the flow direction in the isotropic medium, they would have to be rotated into the permeability coordinates before the transformation to the anisotropic medium is carried out. This will yield off-diagonal terms in D^{ij} and F^{kl} which transform as:

$$d^{12} = d^{21} = \frac{\sqrt{1}}{K_r} \qquad D^{12} = \frac{\sqrt{1}}{K_r} D^{21} \qquad (35a)$$

$$f^{12} = f^{21} = \frac{\sqrt{1}}{K_r} \qquad F^{12} = \frac{\sqrt{1}}{K_r} F^{21} \qquad (36a)$$

Some calculation will show that d^{ij} and f^{kl} are not aligned with either the flow direction or the permeability principal axes in the anisotropic medium. This result is somewhat surprising for the flow factor, but indicates the interaction of the permeability tensor and the confining boundaries.

To prepare for the experimental work, it will be useful to discuss the special cases in which the flow direction is parallel to one of the principal axes of the permeability tensor. First consider the situation in which the velocity is parallel to the major

permeability. As this problem is stated in the permeability coordinates, d^{ij} is given by reference to Eq. 32 and Eq. 35.

$$d_I = A_I F_I + A_{II} F_{II}$$
$$d_{II} = \frac{1}{K_r} (A_{II} F_I + A_I F_{II}) \tag{38}$$

The second case is that in which the velocity is in the same direction as the minor permeability. Now the dispersion coefficient must be rotated through an angle of $\pi/2$ before the transformation can be made, and thus in the isotropic medium in permeability coordinates:

$$D^{11} = D_{II}$$
$$D^{12} = D^{21} = 0 \tag{39}$$
$$D^{22} = D_I$$

when this is transformed into the anisotropic medium the components of d^{ij} are:

$$d^{11} = d_{II}$$
$$d^{12} = d^{21} = 0 \tag{40}$$
$$d^{22} = \frac{1}{K_r} D_I$$

If this is rotated back into the flow or bed coordinates

$$d_I = d^{11} = \frac{1}{K_r} D_I = \frac{1}{K_r} (A_I F_I + A_{II} F_{II})$$
$$d_{II} = d^{22} = D_{II} = (A_{II} F_I + A_I F_{II}) \tag{40a}$$

These transformation formulae will be used in comparing the dispersion measurements in beds which differ only in the angle between the flow and the major axis of the permeability tensor. This will be taken up again in Chapter 4.

3. EXPERIMENTAL APPARATUS AND PROCEDURE

3.1 Apparatus

The experiments were carried out with the apparatus shown schematically in Fig. 3-1. Figure 3-2 is a photograph of the porous bed with the inflow and outflow sections, the manometer board, and the conductivity bridge. The actual tests were done in the porous bed which is shown in the close-up photograph in Fig. 3-3 for bed number 4. Constant head tanks were provided in both the inflow and outflow lines to the porous bed. These head tanks are shown in Fig. 3-4 and Fig. 3-5.

The inflow system included a pump and storage tank so a circulation could be maintained regardless of the quantity flowing through the porous bed. The piezometers in the top and bottom of the bed were connected to individual tubes on the manometer board. A conductivity bridge was used to measure the electrical conductivity of the bed and fluid between pairs of electrodes. The electrodes were mounted in two groups in order to determine the change in tracer distribution during flow through the bed. The flow rate, which was controlled by the head difference across the bed, was determined by time-volume measurements at the discharge head tank.

The central portion of the main apparatus was the packed bed. The packed bed as well as the inflow and outflow sections was made of 1/4 inch Plexiglas. The packed bed was 118 cm long by 30.5 cm high by 76.3 cm wide with a total flow area of 234.5 cm^2. Piezometers with 1/16 inch holes were placed 25.4 cm apart in both the top and bottom of the bed. These were used to obtain the head gradient measurements needed to calculate the permeability. Two sets of electrodes were spaced as shown in Fig. 3-6. The distance between the centers of the two electrode groups was 103 cm. The electrodes were made from stainless steel cap screws. The screws were machined so that a 1/16th inch long by 1/16 inch diameter tip extended into the bed when the screws were in place in tapped holes in the walls of the bed.

The inflow and outflow sections were identical and could be removed when the bed was being packed. Two piezometers were provided in the top and bottom of these sections. The diffuser used in both sections was designed to distribute the inflow laterally and reduce longitudinal entrance velocities to negligible values. The storage tank which had a volume of approximately fifty gallons was used with the pump and inlet head tank to maintain a constant circulation. The Bell and Gosset pump Model P5-6 Size 150 pumped 5 gallons per minute against a static head of 5 feet in a pump test. The two inch diameter overflow weir and discharge pipe was more than adequate for this flow rate, and resulted in almost no change in head throughout the range of flow rate through the bed. The flow rate through the bed ranged form 0.5 cm^3/sec (0.008 gpm) to 21.3 cm^3/sec (0.35 gpm). The outflow head tank discharged into a secondary receiver from which the water could be wasted or, during permeability tests, recycled.

Other equipment included a forty tube manometer board with a useful height of 36 inches. Only eighteen tubes were used. Readings could be obtained to the nearest 0.05 inch or 0.13 cm of water. An Industrial Instruments Model RC-162B2 conductivity bridge with a calibration accuracy of 1% of the reading was used to measure the conductivity of the bed between each pair of electrodes. A conductivity dip cell Type CEL-VS-2 was used to measure the base conductivity of the water. Ancillary equipment included a watch with sweep second hand, graduates, beakers, and a syringe with a number 25 hypodermic needle.

The water used was local tap water which had been treated in an Ilco-Way ion exchange unit. Copper sulfate was added intermittently to control algae growth. The tracer was a solution of 30 grams of sodium chloride in one liter of solution, with the supply water as the solvent. The porous media were two sizes of du Pont "Herox 2" nylon filament. The larger filament had a diameter of 0.020 inch (0.0508 cm) and the smaller filament had a diameter of 0.004 inch (0.01016 cm). The filaments came in bundles, called hanks, which were 46-1/2 inches long and about 2 inches in diameter. This material was selected to provide a high degree of directional effect on the permeability when placed with most of the filaments parallel. It also had to be an electrical insulator and an inert chemical in the dilute salt solution used. Packing was accomplished by slitting the wrapping on each hank before placing, and then removing the wrapper after the material was aligned. There were some filaments, especially in the finer material, which became twisted. The effect of this on the overall packing seemed to be very small, and is discussed in Chapter 4.

3.2 Procedure

Most of the tests were dispersion tests in which the spread of a given amount of tracer was determined as it traveled the length of the bed. A short series of permeability tests was run on each bed before starting the dispersion tests to aid in determining the range of heads and velocities to be expected in that bed.

The procedure for starting or stopping flow either during a test series or at the beginning or end of a series will be described first. At the beginning of a series the three valves shown in Fig. 3-1 were all closed. The pump was started, then the pump valve was opened and circulation established in the supply system. Next the valve on the inlet head tank was opened to apply full head to the bed. Finally, the valve on the outlet head tank was opened to actually start flow through the bed. At the end of a test series this procedure was reversed, though the valve on the inflow head tank was not always closed. During tests the flow was stopped while the electrode conductivities were initially read and the tracer injected at the start of a dispersion test and was started after the reading of the inlet electrode conductivities and was again stopped at the end of the test before the downstream set of electrode conductivities was read. Only the outflow valve needed to be operated for these stoppages, and the time to open or close this valve was about 5 seconds.

Permeability Tests

The outflow constant head tank was fixed to maintain a minimum head of about 1-1/2 ft (40 cm) on top of the bed at all times. The

inflow head tank was then set at an arbitrary elevation above the outflow tank and a period of 10 to 20 minutes allowed before head loss and flow rate measurements were taken. This procedure was repeated until the possible range of Reynolds numbers or head had been covered.

Dispersion Tests

To begin a dispersion test the inflow head tank was set at a pre-determined height above the outflow tank which was set to maintain a minimum pressure head of about 20 cm of water on the bed. After a time of 15 minutes or more for the first test of a series, flow rate and head loss were measured. Then a sample of the outflow fluid was collected to provide the base conductivity measurement and the flow stopped while the electrodes in both sets were read to provide the zero reading. With the flow still stopped, the center electrode on one side of the upstream set was removed and the hypodermic used to inject 1 or 2 cc of the 3% salt solution. Then the upstream set was read again to determine the initial tracer distribution and the flow was started. If the test was long enough the flow rate could be checked and the time between the initial reading at the upstream electrodes and the final reading at the downstream electrodes adjusted if the flow rate had changed from the first measurement. The length of the dispersion tests was calculated by dividing the distance between electrode groups (103 cm) by the seepage velocity. Attempts to determine the time at which the concentration peaked at the downstream electrodes by observing the variation of conductivity as the tracer moved were unsuccessful due to the low concentration observed at this point. At the proper time the flow was stopped and the tracer conductivities measured at the

downstream set of electrodes. After this the flow was again started and, if necessary, another flow rate and head loss determination was made. Several variations in the completion of a test occurred. After the last test of the day and between two tests on one day 1 or 2 pore volumes were allowed to flow through the bed to wash out all of the tracer. If a following test was to be run at a higher velocity the change in the flow rate would be made soon after the completion of the test to speed the flushing. On the other hand, if the next test was to be at a lower velocity, the flow rate would not be changed until after the flushing period.

3.3 Discussion of Procedure

The flow was stopped while the conductivity measurements were being made to determine the tracer distribution at a given time. Bear and Todd (1960) discuss the value of taking measurements at fixed time in contrast to the more common method of measuring at a fixed point with continuing flow. If the flow is steady, the temperature constant, and the bed homogeneous, Eq. 55 could be integrated easily between any two instants of time. On the other hand, if the concentration is measured with time a variable, every reading at each electrode requires different treatment as the rear of the distribution will be longer than the front of the distribution.

But if the flow is started from rest and stopped during the dispersion test there must be a period of unsteady flow. With reference to Hildebrand (1949) the solution for unsteady flow due to a sudden change in head at one end of the bed is found to include the factor

exp $(-n^2\pi^2Ekt/PL^2\mu)$. The following symbols appear only in this expression and are defined here.

n = index of term in series solution

E = bulk modulus of fluid, F/L^2

L = Length of bed, L

With appropriate values for all terms the argument of the exponential function is approximately 10^6n^2t for the 0.02 inch material and approximately 10^5n^2t for the 0.004 inch material. Thus the unsteady flow following a change in head would not extend noticeably beyond the 5 second valve operation time. The total time of unsteady flow during a dispersion test would then be about 10 seconds, which is not more than 2% of the duration of any test. It is felt that unsteady flow may have no direct effect unless the flow reverses direction and increases the total distance traveled. (See Bear and Todd, 1960)

Another possible cause of unsteady flow was the filling and draining of manometer tubes. Considering the tubes to be 3/16 inch in diameter and an average head difference to be 5 inches, a volume change of about 5 cc per manometer tube is indicated. This was observed to take as much as 10 or 15 minutes in the first bed packed with the smaller filaments. Consequently, beginning with tests 2D-11 and 12 the manometers which could cause flow in the vicinity of the downstream electrodes were closed during dispersion runs. Notice that in the plot of data from the tests in bed 2, the horizontal packing of the smaller filaments, these two tests fall well within the general scatter.

3.4 Discussion of Experiments

The various problems which arose during the experimental program are mentioned and discussed here. Originally the tracer was to have been introduced through a tube ending in a diffuser across the center of the upstream face of the packed bed. The diffuser was not designed correctly for the laminar flow which occurred in the tube. However, correction of the diffuser design would not have improved results. If the tracer was introduced into the 4 ft long tube in a slug, the dispersion in the tube resulted in a very long, dilute tracer distribution before the slug ever reached the diffuser or the bed. Attempts to have the tube full of tracer solution failed, and would have required a delicate valve inside the main apparatus. Thus the hypodermic injection was adopted as a second choice. The volume injected was selected with the idea of obtaining as nearly two-dimensional initial conditions as possible.

Some trouble was experienced in packing the beds as evidenced by the increase in porosity with each bed packed. No solution seemed possible except to have had a stronger box and an arrangement to obtain better compaction of the filaments. End screens were needed to contain the vertical packing and were held in place by friction (See Fig. 3-3). They should have had negligible effect on the flow and were not in a region in which measurements were taken.

A non-uniform head loss near the entrance to bed 1 was noted during later tests. This bed was in place for about 5 months and the entrance became packed with algae which grew in the early water supply

despite treatment with copper sulphate. This area did not extend to the upstream electrode set so was ignored in the dispersion tests and was handled in permeability calculations by omitting the first piezometer pair. The problem of algae growth decreased as the tests proceeded on to new beds and water. Apparently the ion exchange equipment had been only lightly used for some time prior to the start of this program and had become contaminated by the algae. Once the source of algae was thoroughly flushed the problem was solved.

The second bed caused no problems except that the finer filaments were considerably more difficult to handle. Bed 3 was also no problem except that the downstream screen moved out about 1 cm because of poor packing and an excessive head difference. This affected only the very end of the bed downstream of any measurement.

Bed 4 gave no results for the first several dispersion tests. Then a gap between the top of the filaments and the top of the bed was detected and verified by dye injection. Most of the flow was short-circuiting through this space. This was remedied by installing one-quarter inch foam rubber along the top of the bed. Breaks were provided in the rubber so the top piezometers could still be used.

4. DATA ANALYSIS

4.1 Data Reduction

The flow rate and head loss data constitute a set of data from which permeability, time of dispersion tests, and Reynolds numbers could be calculated. The conductivity data could be reduced to concentration values and then to standard deviations for the tracer distribution.

The permeability calculations proceed as follows:

$$u = V/tPA \tag{41}$$

where: V = volume collected in time t

A = total flow area

If Eq. 7 is written in finite form for one component, it may be solved to yield:

$$k = Pu\mu/\gamma(\Delta h/L) \tag{42}$$

where: Δh = head loss in length L

The Reynolds number may also be determined:

$$Re = ud/\nu \tag{43}$$

The Peclet number, in terms of the effective molecular diffusivity is:

$$Pe = ud/D_m \tag{44}$$

The conductivity data requires considerably more calculation. The end results are the dispersion coefficients, though in this section only the standard deviations of the tracer distribution are computed. The basic equation for specific conductance is given in terms of measured conductivity, the cell constant, and a temperature correction.

$$1/\rho = \frac{B}{(1 + 0.025\Delta T)R} \tag{45}$$

where: $1/\rho$ = specific conductance at 25°C (micromhos/cm)

$1/R$ = measured conductance (micromhos)

B = cell constant (1/cm)

ΔT = temperature difference, (T-25)

Since each pair of electrodes can have a different cell constant because of bed configuration and manufacturing tolerance between electrodes, a reference specific conductance is obtained from the unmarked fluid by use of the calibrated dip cell.

$$1/\rho_o = \frac{B}{(1 + 0.025\Delta T)R_o} \tag{45a}$$

When each electrode pair is read before introducing the tracer, an electrode constant, B', can be calculated from Eq. 45.

$$B' = (1/\rho_o)\, R'\, (1 + 0.025\Delta T) \tag{46}$$

Since each component of the solution is in parallel with the rest of the solution, the measured conductivity and specific conductance add (if the temperature is constant):

$$\frac{1}{\rho} = \frac{1}{\rho_o} + \frac{1}{\rho_c} \tag{47}$$

where: $1/\rho_c$ is the specific conductance of the salt concentration

But $$1/\rho = \frac{B}{(1 + 0.025\Delta T)R} \tag{48}$$

and therefore $$1/\rho_c = (1/R - 1/R') \frac{B'}{(1 + 0.025\Delta T)} \tag{49}$$

Now substitute for B' from Eq. 46:

$$1/\rho_c = 1/\rho_o \, (1/R - 1/R')/(1/R') \tag{50}$$

And a final substitution for $1/\rho_o$ from Eq. 45a:

$$1/\rho_c = \frac{R'}{R_o} \left(\frac{1}{R} - \frac{1}{R'}\right) \frac{B}{(1 + 0.025\ \Delta T)} \tag{51}$$

The relation between $1/\rho_c$ and the concentration was determined by successive dilution in distilled water with the dip cell used to measure the conductance. The concentration for the dispersion tests were obtained by means of Fig. 4-1 and the results of calculations using Eq. 51.

The concentrations were then used to calculate the standard deviations of the tracer distribution, by means of the least squares method. The curve fitted to the data was the normal distribution

function. In most cases the centroid of the electrode group was also the centroid of the tracer distribution. This simplified the calculations as the distance to each electrode was a constant for all tests. The equations for the least squares analysis were set up independently for the points on the x and y axes. The equations for the normal distribution curves are:

$$c(x, 0) = (c_o/2\sigma_x\sigma_y) \exp - (x^2/2\sigma_x^2)$$

$$c(0, y) = (c_o/2\sigma_x\sigma_y) \exp - (y^2/2\sigma_y^2) \qquad (52)$$

The least squares equations for the x direction are:

$$N\log a - b\Sigma(x^2)_i = \Sigma\log c(x_i,0)$$

$$-\log a\Sigma(x^2)_i + b\Sigma(x^4)_i = -\Sigma(x^2)_i \log c(x_i,0) \qquad (53)$$

where: $a = c_o/2\sigma_x\sigma_y$, $b = 1/2\sigma_x^2$

c_o = reference concentration

σ_x, σ_y = standard deviations of the tracer distribution

N = number of points

Note that the coefficients of loga and b on the left side of these equations depend only on the number and spacing of points at which measurements were taken. Since these were fixed at each set of electrodes it is convenient to express distance in terms of the electrode spacing (0.5 inch or 1.27 cm), and to solve the two equations for loga and b by Cramer's rule. Thus:

$$\log a = ((\Sigma x^4)(\Sigma\log c) - (\Sigma x^2)(\Sigma x^2 \log c))/D$$

$$b = (N(-\Sigma x^2 \log c) - (-\Sigma\log c)(\Sigma x^2))/D \qquad (54)$$

where: $D = N(\Sigma x^4) - (\Sigma x^2)^2$

The values of Σx^2, Σx^4, and D are given in Table 4-1 for the three values of N occurring in the electrode groups. Most of the multiplication and division was done on a slide rule. The basic data do not warrant more accuracy. In some tests the data not on the axes of the electrode groups were used to adjust the values used to obtain real values for the standard deviations.

4.2 Presentation of Results

The standard deviations of the tracer distribution obtained from the conductivity data permit the calculation of the longitudinal and lateral dispersion coefficients. Bear and Todd (1960) discuss the relation between the tensor of variance of the tracer distribution and the tensor dispersion coefficient. If the convective-duffusion equation is written in moving coordinates to eliminate the convective terms, it can be shown that:

$$\frac{d(\sigma^2)^{ij}}{dt} = 2D^{ij} \tag{55}$$

If this equation is expressed in finite form, the components of D^{ij} can be obtained from the experimental change in variance and elapsed time. With reference to Eqs. 39 and 55, the dispersion coefficient has the components:

$$d_I = \frac{\Delta(\sigma_x^2)}{2\Delta t}$$
$$d_{II} = \frac{\Delta(\sigma_y^2)}{2\Delta t} \tag{56}$$

for the case in which the flow and major permeability are parallel.

There is some difference of opinion as to the proper or best manner of presenting and correlating dispersion test results. Hawley (1964) presents a plot of a Peclet number, ud/D, as ordinate with the Reynolds number, ud/ν as abscissa. Collins (1961) plots D/D_m against ud/D_m but does not mention the Reynolds number of the flows. Harleman et al (1963) chose to present D/ν as a function of the Reynolds number. As discussed in section 2.3, the chosen parameters for this study are D/D_m and ud/D_m. Thus the results will show the functional relation between the ratio of the dispersion coefficient to the effective molecular diffusivity and the Peclet number. The use of the kinematic viscosity as a reference property is not recommended for two reasons. First, the kinematic viscosity depends inversely on temperature while the molecular diffusivity depends directly on temperature. Second, viscosity does not appear in the convective diffusion equation which has been assumed to describe the dispersion process if the correct coefficient is used. A paper by Benson (1965) on the danger of obtaining false correlations from dimensionless plots casts doubt on the significance of the Peclet versus Reynolds number plot, at least if only laminar flow is considered.

Plots of kinematic viscosity and molecular diffusivity as functions of temperature are shown in Fig. 4-2. The effective molecular diffusivity is obtained by multiplying the molecular diffusivity from Fig. 4-2 by the factor (2P)/(3 - P), which is taken from the work by Bell and Grosberg (1961). Values of this factor, the porosity, permeability, size and orientation of the bed material, and range of Re, Pe, and temperature for each bed are listed in Table 4-2. Tables

4-3 through 4-6 present the results of the successful dispersion tests. Tests with "DT" run numbers were performed in the first bed of each orientation to determine good test procedure. Data given for each run include temperature, seepage velocity, time of dispersion test, Pe, Re, D_x and D_y. The notation D_x will always refer to experimental results, while d_I might be the appropriate symbol for the same tensor component in Chapter 2. The data is presented graphically in Figs. 4-3a through 4-6b. The longitudinal or x component is presented in part a of each figure and the lateral or y component is presented in part b.

The lines shown in these figures were obtained by the least squares method and the equations of these lines are listed in Table 4-7. In the case of bed 2 the scatter in the results for D_x/D_m are too great and the least squares line is unreasonable when compared to the other tests. The line used was determined from the other results as follows. In beds 1, 3, and 4 the exponents of the ratio D_x/D_y are 0.50, 0.48, and 0.31, respectively. Comparing between beds, the exponent of the ratio of D_x in bed 1 to D_x in bed 3 is 0.23, and the ratio of y components has the exponent 0.21 for beds 1 and 3, and 0.22 for beds 2 and 4. The exponent in the equation for D_x/D_m in bed 2 was made to conform to these comparative ratios and the coefficient was chosen so the line would pass through the centroid of the data. The quality of the least squares lines and of visually fitted lines is discussed in the appendix.

A composite plot of the equations in Table 4-6 is presented in Fig. 4-7. For comparative purposes results of tests reported by Harleman and Rumer (1962) are also shown. Their original graph had the

Reynolds number as the abscissa. The Reynolds number may be multiplied by ν/D_m to give the Peclet number. For their tests the effective molecular diffusivity was $0.47(10)^{-5}$ cm^2/sec and the kinematic viscosity was about $0.92(10)^{-2}$ cm^2/sec, so Pe = 1960 Re. These tests were conducted in isotropic beds packed with plastic beads 0.096 cm in diameter. The longitudinal or D_x values were obtained from displacement tests in a vertical column, but the lateral or D_y values were obtained in steady state tests of dispersion between fresh and salt water layers in a rectangular, horizontal bed.

4.3 Discussion of Results

As mentioned in section 2.3, the results of dispersion tests in the same size but differently oriented material may be transformed into an isotropic porous medium for comparison with each other or with other experiments in isotropic media. Before this can be done, both components of the permeability must be known. The principal values of the permeability were measured in separate beds. However, due to difficulty in packing the beds there was a variation in porosity from bed to bed. The permeabilities may be corrected for the difference in porosity by means of the Kozeny equation (Collins, 1961) which states that:

$$k \propto P^3/\Sigma^2 \qquad (58)$$

If it is desired to relate results in the two sizes of material the specific surface may be replaced by 1/d for comparative work. For beds of different porosity but the same size material, the permeability

ratio between beds, becomes, for example:

$$k_1/k_3 = (P_1/P_3)^3 \tag{58}$$

If this equation is applied to the experimental values in Table 4-2, the results are as given in Table 4-8. Only the permeability ratio, not the magnitude of k_I, appears in the transformation of Eqs. 38 and 40. It would seem reasonable to make the comparisons in a porous medium of the same permeability. However, an attempt to do this will not affect the results of transforming the dispersion tensor since the permeability ratio in one bed or a pair of beds would not be changed. The results of the transformation from the anisotropic porous media of the tests into isotropic media are shown in Table 4-9. Note that only the coefficients are changed. The exponents are not affected at all by the transformation so further comparison is not simplified.

In fact, the variable exponent might seem to be a block to any analysis. On the other hand, this phenomenon has been suggested and reported only by Harleman and Rumer (1962). The present experiments verify the occurrence of this phenomenon and give some hint of the mechanism. If the theory of Taylor (1953) for dispersion in circular tubes is adapted to porous media flow in the same manner as flow in tubes is adapted in the "capillary bundle" theory, then the dispersion coefficient should be proportional to the square of the velocity. But, if the statistical theories proposed by Saffman (1960) and De Jong (1958) and the "cell" theory of Bear and Todd (1960) are accepted, the dispersion coefficient should be proportional to the first power of the velocity. Most experimenters report exponents of approximately 1.2 for

the longitudinal component. (See Collins, 1961 and Harleman and Rumer, 1962). The only report of an expression for the lateral component available is that of Harleman and Rumer (1962). They obtain an exponent less than 1 in their expression for lateral dispersion. This result is paralleled by bed 4 of the present study.

The variable exponent does raise severe questions about the development leading to Eq. 38. If the equations describing the results in bed 1 are considered, several problems become apparent. The transformations used in obtaining the equations in Table 4-9 are the inverse of the one in Eq. 38. Thus in the isotropic medium corresponding to bed 1:

$$D_I/D_m = d_I/D_m = A_I F_I + A_{II} F_{II} = 0.0017 Pe^{1.85} \tag{59}$$

and $$D_{II}/D_m = K_r \; d_{II}/D_m = K_r \; (A_{II} F_I + A_I F_{II}) = 0.136 \; Pe^{1.35}$$

The work of Bear and Todd (1960), Scheidegger (1961) and Harleman and Rumer (1962) all indicate that F_{II} should be zero for the case in bed 1. This assumption leaves F_I with different exponents in different components of D^{ij}. If $F_I = Pe^{1.85}$ and $F_{II} = Pe^{1.35}$, A_{II} should be zero, but A_I is not the same in two components of D^{ij}. Similar anomalies occur for all four beds as well as for the data Harleman and Rumer (1962) when it is put in this form.

Two possible answers to the problems apparent above will be discussed. The choice between them, or the possibility of other alternatives, is left to future study. The first possibility is to

preserve the hypothesis of Eq. 27 by introducing a more general expression for F^{kl}. The simplest function to replace the exponential one used is a polynomial. Thus, if a second degree relation is desired, F^{kl} takes on the form:

$$F^{kl} = a^{kl} + b^{kl}u + c^{kl}u^2 \tag{60}$$

F^{kl} may still be assumed to be symmetric. The experimental results would be fitted by a curve with the form of:

$$D/D_m = A + BPe + CPe^2 \tag{61}$$

Several restrictions are necessary to obtain reasonable curves. First, since $D = D_m$ when $Pe = 0$, A must be equal to 1. Second, negative values of D/D_m are physically meaningless. In trying to use this type of equation, the only way to satisfy the second restriction was to require zero slope at $Pe = 0$. This resulted in an equation of the form:

$$D/D_m = 1 + CPe^2 \tag{62}$$

This appears too limited in light of the available empirical results. If the linear term can be retained along with the restriction against negative values of D/D_m, this may permit the original hypothesis to be used.

The other possible way to handle the problem is to propose another hypothesis on the relation between D^{ij} and F^{kl}. Along with a new expression for D^{ij}, several statements will be made on the mechanism resulting in the variable exponent. There can be no argument with the definition of the dispersion coefficient in terms of the symmetric

second rank tensor appearing in the convective-diffusion equation. Thus D^{ij} is still given by Eq. 29 in an isotropic medium, or in its principal axis system in an anisotropic medium. The following form is proposed for the dependence of the dispersion tensor on the porous medium and the flow:

$$D^{ij} = A^i_m F^{jm} \tag{63}$$

where: A^i_m is a function of the porous medium

F^{jm} is a function of the flow

This is similar to the relation in Eq. 27, except that the tensor describing porous medium is now a mixed second rank tensor instead of a mixed fourth rank tensor. If this relation is written out, it yields:

$$\begin{aligned} D^{11} &= A^1_1 F^{11} + A^1_2 F^{12} \\ D^{12} &= A^1_1 F^{21} + A^1_2 F^{22} \\ D^{21} &= A^2_1 F^{11} + A^2_2 F^{12} \\ D^{22} &= A^2_1 F^{21} + A^2_2 F^{22} \end{aligned} \tag{63a}$$

in the isotropic medium. If D^{ij} and F^{jm} are symmetric and have their major principal axes aligned with the flow as assumed in section 2.3 then:

$$D^{12} = A^1_2 F^{22} = D^{21} = A^2_1 F^{11} = 0 \tag{64}$$

This requires that $A^1_2 = A^2_1 = 0$, so A^i_m is also symmetric with the same principal axes as D^{ij} and F^j_m. If the flow in the isotropic medium is

not aligned with a permeability axis from the anisotropic medium, then all three second rank tensors must be rotated into permeability coordinates before the transformation to the anisotropic medium may be applied. When this transformation is carried out, the mixed tensor, A_m^i transforms as follows:

$$\begin{aligned} a_1^1 &= A_1^1 \\ a_2^1 &= \sqrt{K_r}\, A_2^1 \\ a_1^2 &= \frac{\sqrt{1}}{K_r}\, A_1^2 \\ a_2^2 &= A_2^2 \end{aligned} \tag{65}$$

Now d^{ij} may be written in terms of A_m^i and F^{jm} as:

$$\begin{aligned} d^{11} &= D^{11} = A_1^1 F^{11} + A_2^1 F^{12} \\ d^{12} &= \frac{\sqrt{1}}{K_r}\, D^{12} = \frac{\sqrt{1}}{K_r}\,(A_1^1 F^{21} + A_2^1 F^{22}) \\ d^{21} &= \frac{\sqrt{1}}{K_r}\, D^{21} = \frac{\sqrt{1}}{K_r}\,(A_1^2 F^{11} + A_2^2 F^{12}) \\ d^{22} &= \frac{1}{K_r}\, D^{22} = \frac{1}{K_r}\,(A_1^2 D^{21} + A_2^2 F^{22}) \end{aligned} \tag{66}$$

For the case in which the flow and major permeability are parallel in the anisotropic medium this simplifies to:

$$\begin{aligned} d^{11} &= d_I = D_I = A_1^1 F_I \\ d^{22} &= d_{II} = \frac{1}{K_r}\, D_{II} = \frac{1}{K_r}\, A_2^2 F_{II} \\ d^{12} &= d^{21} = 0 \end{aligned} \tag{67}$$

For the case in which the flow is perpendicular to the major permeability in the anisotropic medium this simplifies to:

$$d^{11} = d_I = \frac{1}{K_r} D_I = \frac{1}{K_r} A_1^1 F_I$$

$$d^{22} = d_{II} = D_{II} = A_2^2 F_{II} \qquad (68)$$

$$d^{12} = d^{21} = 0$$

These equations are compatible with the experimental results. However, little information can be gained by use of Eqs. 67 and 68.

The experimental results are presented so as to make F^{jm} appear to be equal to $(Pe^n)^{jm}$, where the exponent varies from component to component but the argument does not change. The coefficient A_m^i depends on the solid and fluid phases. The exponent depends in some complex way on the pore geometry. As previously noted, theoretical studies of dispersion have resulted in exponents of either 1 or 2. It is proposed that the exponent is a function of the angle between the flow and major principal axis of the permeability tensor, of the directness or tortuosity of the flow channels, and of the component itself. A porous medium with fairly straight flow channels and the flow and major permeability parallel would have an exponent in the expression for the longitudinal component of the dispersion coefficient which would be near 2. The lateral component in the same medium would have a smaller exponent. On the other extreme, a perfectly random packing should have an exponent near 1 in the longitudinal component and have an exponent less than 1 in the lateral component.

5. CONCLUSIONS

The original plan of this study had been to take the existing theory of dispersion in isotropic porous media and adapt it to anisotropic porous media by use of the transformation commonly applied in flow problems. The statement that $D^{ij} = A^{ij}{}_{kl}F^{kl}$ was recognized as an hypothesis, not as an established fact. The early efforts at analyzing the experimental results pointed to severe difficulties with this relation. After some reconsideration of the proper parameters to use in analyzing the data, the contradiction between this theory and the experimental evidence became more apparent, as is described in section 4.3. Thus the first conclusion is that the expression above, combined with an exponential plot of experimental results is not correct. The theory might be saved by using a polynomial relation for F^{kl} in terms of the velocity. This is compatible with the theories for one-dimensional dispersion, but it is contrary to the work of other experimenters in this area.

A more positive conclusion is the verification of the assertion by Harleman and Rumer that the exponents in the flow factor are different for different components. This is, in fact, the main reason the original theory fails.

An effort to devise a combination of two tensors that would represent D^{ij} as given by experiment was then necessary. This resulted in Eq. 63: $D^{ij} = A^{i}_{m}F^{jm}$. The relation between these three tensors is

quite different from the relation of Eq. 27. Now the flow factor is directly identified with the dispersion coefficient in one index and is identified with only one of two indices on the medium tensor. The medium tensor is symmetric in an isotropic medium, which is less restrictive than the requirement in the previous theory that the fourth rank tensor be isotropic. Several statements about the factors affecting the exponent on the flow factor can be made from the experimental results. In a power relation like the present one, the exponent is the dominating term, especially since the argument is the same in all components. It is postulated that the exponent depends on three things: (1) angle between the flow and major permeability, (2) flow path geometry through the pore space, (3) the component.

More conclusive results must wait upon further research. The problem is very complex and many ways are open to examination. Several possibilities offer some chance of success, including: (1) experiments similar to the ones in this study in different media, either isotropic or anisotropic, (2) dispersion experiments using the Hele-Shaw model of the porous medium, (3) mathematical investigation of the nature of the dispersion process. Whatever the direction of experimental work, the use of more precise instrumentation is required. This is particularly true when physical properties other than diffusivity are excluded since this limits the tracer concentrations to very small values.

Quantitative practical application of the theoretical and empirical studies of the fundamental nature of the dispersion process in flow through porous media is still in the future. The immediate need

is for research to provide a definite indication of the proper theory to describe the dispersion process. After the correct theory is determined, emphasis can be placed on the properties of porous media; especially of natural deposits where the significant dispersion related problems occur.

A P P E N D I C E S

A P P E N D I X

Least Squares Analysis of Data

The existing theories postulate and the available experiments support the correctness of a relation such as $D = AV^n$. Following this trend, the present data is presented on log-log plots and a straight line is fitted through the data. Due to the spread of the data, the least squares method was selected to determine the equation of the plotted lines. The range of validity of these lines should be noted carefully. If the Peclet number is less than about 0.1 (Collins, 1961) the ratio of D/D_m is constant. Consequently for Peclet numbers between 0.1 and about 10 the relation is non-linear as the slope increases from zero to a value between 1 and 2 as the Peclet number increases. The upper limit for these lines is not clearly defined, but will depend on a transition from laminar to turbulent diffusion.

The least squares analysis of each set of data is carried out on the logarithmic form of the exponential relation:

$$\log D/D_m = \log A + n\,\mathrm{Log}Pe \tag{69}$$

The simultaneous equations for logA and n are:

$$\begin{aligned} N\log A + n\Sigma\log Pe &= \Sigma\log(D/D_m) \\ \log A\Sigma\log Pe + n\Sigma(\log Pe)^2 &= \Sigma(\log Pe \log D/D_m) \end{aligned} \tag{70}$$

Where: A = coefficient of Pe^n

n = exponent on Pe

N = number of data points

The lines determined by these equations will be the best fit in a least squares sense; that is, the sum of the squared differences between the data and the line is minimized.

However, for some of the graphs, especially Figs. 4-3b, 4-5a, and 4-6a, inspection would suggest that a steeper slope would provide a better fit than the least squares line. In order to verify the least squares lines and check the visually fitted lines, the sum of the squared differences were calculated. For each graph the least squares line, the visual line and at least one other line were selected for this computation. All lines pass through the centroid of the data so selection of the slope determined each line. The results are presented in terms of the root mean square difference, which is simply the square root of the mean of the squared differences. Tables A-1 to A-4 list the slope of each line, the actual value of the root mean square difference (R), and the ratio of each of these to the respective value for the least squares line. The relative results are presented graphically in Figs. A-1 to A-4. As an indication of the shape of the curves in these figures, the difference between the high and low slope ratio at a root mean square difference 5 percent higher than the minimum is also given in Tables A-1 to A-4. From this computation, the lines in Figs. 4-3a, 4-4b, 4-5b, and 4-6b are relatively good fits as a moderate change in slope causes a significant increase in the difference. The reason for the steeper visually chosen slopes in several cases is also evident.

For instance, in Fig. 4-3b, the visually selected slope of 1.85 is 1.37 times the least squares line slope of 1.35 but the root mean square difference is increased by only 2 percent. In Fig. 4-5a, the visually selected line has a slope of 1.30 times the least squares slope and increases the difference by 5 percent, and in Fig. 4-6a a slope of 1.52 times the least square slope is needed to increase the difference by 5 percent and the visual slope of 2.15 is 1.89 times the least square slope yet has a difference just 15 percent larger. However, from Fig. A-3, the line chosen for Fig. 4-4a by comparison with the other fitted lines is not a good fit in the least squares sense.

This completes the discussion of the quality of the fitted lines. There are no gross errors in the least squares analysis though the minimum is not particularly sharp for half of the graphs. The difference between the least squares lines and visually selected lines points out a difference between the methods. The least squares method satisfies a mathematical condition while the visually method tries to put the line as close to as many points as possible, especially near the ends of the range.

The significance of the lines, especially of the slopes, is discussed in the section 4.3. Even if the spread of the data raises some question about the numerical value of some of these slopes, the fact remains that they differ from bed to bed and from orientation to orientation.

TABLE 4 - 1

PARAMETERS IN LEAST SQUARES

ANALYSIS OF TRACER DISTRIBUTION

N	Σx^2	Σx^4	D
3	2	2	2
5	10	34	70
7	28	196	588

TABLE 4 - 2

SUMMARY OF EXPERIMENTAL WORK

Bed Number	1	2	3	4
d, cm	0.0508	0.0102	0.0509	0.0102
Orientation	H	H	V	V
P	0.30	0.35	0.35	0.41
$\frac{2P}{3-P}$	0.22	0.26	0.26	0.32
k, cm^2	$1.01(10)^{-5}$	$0.18(10)^{-5}$	$0.76(10)^{-5}$	$0.058(10)^{-5}$
Re, min	0.15	0.008	0.16	0.014
Re, max	1.30	0.20	1.54	0.085
Pe, min	426	15	370	27
Pe, max	3550	397	3000	151
T, ^oC, min	22.5	24.4	23.4	23.1
T, ^oC, max	23.4	27.5	27.0	24.6

TABLE 4 - 3

DATA FOR BED 1.

Run No.	T, °C	u cm/sec	Re	t sec	Pe	$\frac{Dx}{Dm}$	$\frac{Dy}{Dm}$
DT-7	23.0	0.184	0.96	515	2685	2310	824
DT-10	23.0	0.138	0.75	510	2100	4060	960
DT-11	23.0	0.136	0.74	690	2070	1060	1020
DT-12	23.0	0.135	0.74	737	2070	4070	802
D-3	22.5	0.050	0.27	2070	774	308	231
D-5	22.5	0.087	0.46	1165	1320	625	1210
D-6	22.9	0.118	0.64	895	1790	2020	4800
D-7	23.1	0.174	0.95	605	2680	2500	5030
D-8	23.4	0.233	1.30	445	3550	9690	2830
D-9	23.3	0.199	1.09	505	2980	4760	4660
D-11	23.0	0.095	0.52	1060	1450	1750	3170
D-12	23.0	0.055	0.30	1810	838	263	317
D-13	23.7	0.027	0.15	3865	426	227	136

TABLE 4 - 4

DATA FOR BED 2.

Run No.	T °C	u cm/sec	Re	t sec	Pe	Dx/Dm	Dy/Dm
D-1	24.4	0.0576	0.065	1800	136	109	167
D-2	27.5	0.0065	0.008	10,780	15	72	15
D-3	27.1	0.0113	0.014	9120	27	327	73
D-5	25.7	0.0287	0.034	3600	70	342	109
D-6	26.0	0.0612	0.072	1675	148	494	148
D-8	26.1	0.1096	0.13	932	264	483	408
D-9	26.6	0.1698	0.20	607	397	1280	638
D-11	25.4	0.0696	0.080	1485	167	606	650
D-12	25.5	0.0387	0.045	2683	93	206	76

TABLE 4 - 5

DATA FOR BED 3.

Run No.	T °C	u cm/sec	Re	t sec	Pe	$\frac{Dx}{Dm}$	$\frac{Dy}{Dm}$
DT-1	24.0	0.131	0.72	790	1630	1850	1440
DT-2	24.0	0.130	0.72	805	1630	222	658
D-1	27.0	0.070	0.42	1495	817	362	264
D-3	27.0	0.162	0.97	636	1890	3870	506
D-4	27.0	0.210	1.26	487	2450	1090	732
D-5	27.0	0.258	1.54	400	3000	2910	722
D-6	27.0	0.177	1.06	580	2060	1890	1470
D-7	23.9	0.151	0.84	680	1920	12,250	496
D-9	23.4	0.057	0.31	1820	735	366	171
D-11	24.8	0.224	1.27	460	2750	782	875
D-12	23.7	0.029	0.16	3526	370	70	93

TABLE 4 - 6

DATA FOR BED 4.

Run No.	T °C	u cm/sec	Re	t sec	Pe	Dx/Dm	Dy/Dm
D-1	23.6	0.0662	0.072	1555	133	4400	178
D-2	24.2	0.0532	0.058	1930	108	760	117
D-3	23.4	0.0200	0.022	5152	42	82	49
D-4	23.8	0.0429	0.047	2400	88	279	88
D-5	23.1	0.0312	0.134	3310	66	133	79
D-6	23.2	0.0127	0.14	8210	27	170	39
D-7	23.9	0.0652	0.072	1569	133	161	113
D-8	23.3	0.0355	0.038	2891	73	459	64
D-10	24.6	0.0511	0.057	2005	102	294	120
D-11	24.6	0.0758	0.085	1339	151	1480	205
D-12	23.1	0.0224	0.024	4623	47	775	88

TABLE 4 - 7

EQUATIONS OF LINES FIT TO DATA BY LEAST SQUARES METHOD

Bed and Direction	Equation
1-x	$\frac{Dx}{Dm} = 0.0017Pe^{1.85}$
1-y	$\frac{Dy}{Dm} = 0.058Pe^{1.35}$
2-x	$\frac{Dx}{Dm} = 0.647Pe^{1.35}$
2-y	$\frac{Dy}{Dm} = 1.19Pe^{1.05}$
3-x	$\frac{Dx}{Dm} = 0.0074Pe^{1.62}$
3-y	$\frac{Dy}{Dm} = 0.127Pe^{1.14}$
4-x	$\frac{Dx}{Dm} = 2.74Pe^{1.14}$
4-y	$\frac{Dy}{Dm} = 2.54Pe^{0.83}$

Harleman and Rumer	Equation
x	$0.191Pe^{1.18}$
y	$0.55Pe^{0.65}$

TABLE 4 - 8

ANISOTROPIC PERMEABILITIES

Bed	$k_{I,\ cm^2}$	k_{II,cm^2}	$K_r = \frac{k_I}{k_{II}}$
1	$1.014(10)^{-5}$	$0.476(10)^{-5}$	2.14
2	$0.178(10)^{-5}$	$0.036(10)^{-5}$	4.95
3	$1.613(10)^{-5}$	$0.757(10)^{-5}$	2.14
4	$0.287(10)^{-5}$	$0.058(10)^{-5}$	4.95

TABLE 4 - 9

TRANSFORMED DISPERSION COEFFICIENTS

Bed	$\frac{Dx}{Dm}$	$\frac{D_I}{Dm}$	$\frac{Dy}{Dm}$	$\frac{D_{II}}{Dm}$
1	$0.0017Pe^{1.85}$	$0.0017Pe^{1.85}$	$0.058Pe^{1.35}$	$0.124Pe^{1.35}$
3	$0.0074Pe^{1.62}$	$0.162Pe^{1.62}$	$0.127Pe^{1.14}$	$0.127Pe^{1.14}$
2	$0.647Pe^{1.35}$	$0.647Pe^{1.35}$	$1.19Pe^{1.05}$	$5.89Pe^{1.05}$
4	$2.74Pe^{1.14}$	$13.57Pe^{1.14}$	$2.54Pe^{0.83}$	$2.54Pe^{0.83}$

TABLE A - 1

SUMMARY OF LEAST SQUARES CHECK COMPUTATION

Bed 1

Orientation	X		Y	
Quantity	Value	Ratio	Value	Ratio
Slope, S	1.35	0.73	0.85	0.63
	1.85 L.S.	1.00	1.35 L.S.	1.00
	2.34 eye	1.27	1.85 eye	1.37
			2.00	1.48
Root mean square difference, R	0.54	1.15	0.82	1.13
	0.47	1.00	0.73	1.00
	0.57	1.21	0.74	1.02
			0.76	1.05
Spread of slope ratio at $R/R_{LS} = 1.05$		0.40		0.78

TABLE A - 2

SUMMARY OF LEAST SQUARES CHECK COMPUTATION

Bed 2

Orientation	X		Y	
Quantity	Value	Ratio	Value	Ratio
Slope, S.	0.50	0.83	0.87	0.83
	0.60 L.S.	1.00	1.05 L.S.	1.00
	0.96	1.60	1.24 eye	1.18
	1.35 eye	2.25		
Root mean square difference, R	0.60	1.02	0.50	1.07
	0.59	1.00	0.47	1.00
	0.68	1.15	0.49	1.03
	0.90	1.52		
Spread of slope ratio at $R/R_{LS} = 1.05$		0.58		0.36

TABLE A - 3

SUMMARY OF LEAST SQUARES CHECK COMPUTATION

Bed 3

Orientation	X		Y	
Quantity	Value	Ratio	Value	Ratio
	1.28	0.79	0.93	0.82
Slope, S	1.62 L.S.	1.00	1.14 L.S.	1.00
	2.10 eye	1.30	1.41 eye	1.24
Root mean	1.01	1.02	0.49	1.20
square difference,	0.98	1.00	0.41	1.00
R	1.03	1.04	0.44	1.08
Spread of slope ratio at $R/R_{LS} = 1.05$		0.60		0.36

TABLE A - 4

SUMMARY OF LEAST SQUARES CHECK COMPUTATION

Bed 4

Orientation	X		Y	
Quantity	Value	Ratio	Value	Ratio
Slope, S	1.00	0.88	0.66	0.80
	1.14 L.S.	1.00	0.83 L.S.	1.00
	1.50	1.32	1.00 eye	1.20
	2.15 eye	1.89		
Root mean square difference, R	0.99	1.04	0.22	1.09
	0.95	1.00	0.20	1.00
	0.97	1.02	0.22	1.08
	1.09	1.15		
Spread of slope ratio at $R/R_{LS} = 1.05$		0.65		0.34

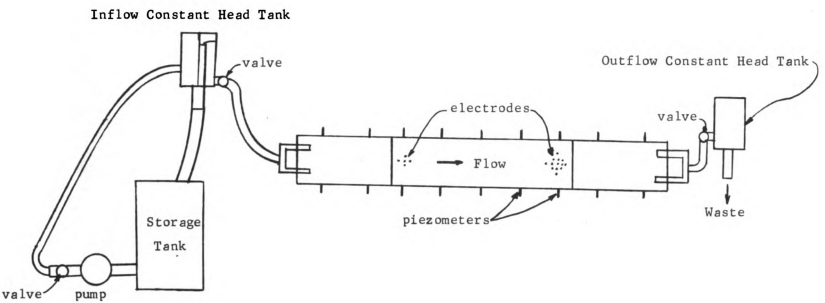

Fig. 3-1 General Layout of Porous Bed

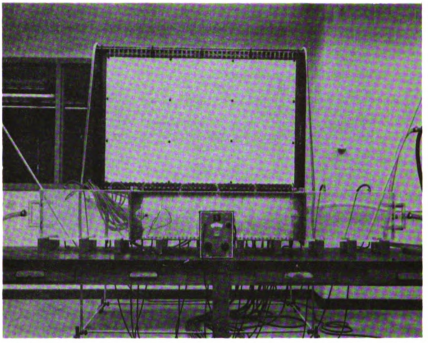

Fig. 3-2 Overall View of Apparatus

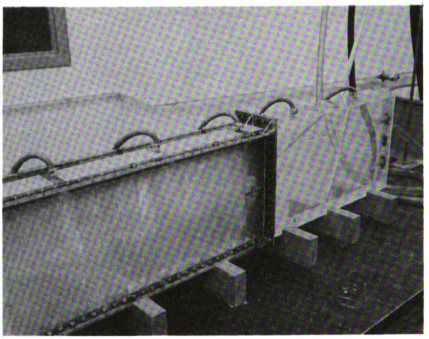

Fig. 3-3 Porous Bed and Electrode Group

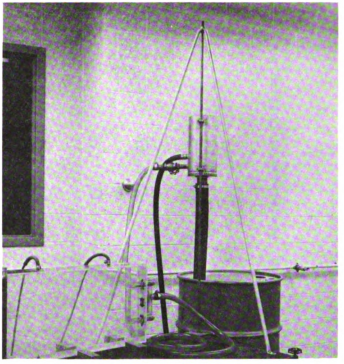

Fig. 3-4 Inlet Constant Head Tank

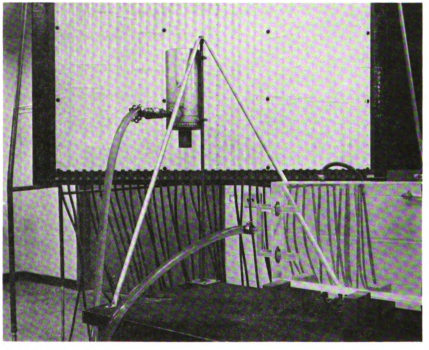

Fig. 3-5 Outlet Constant Head Tank

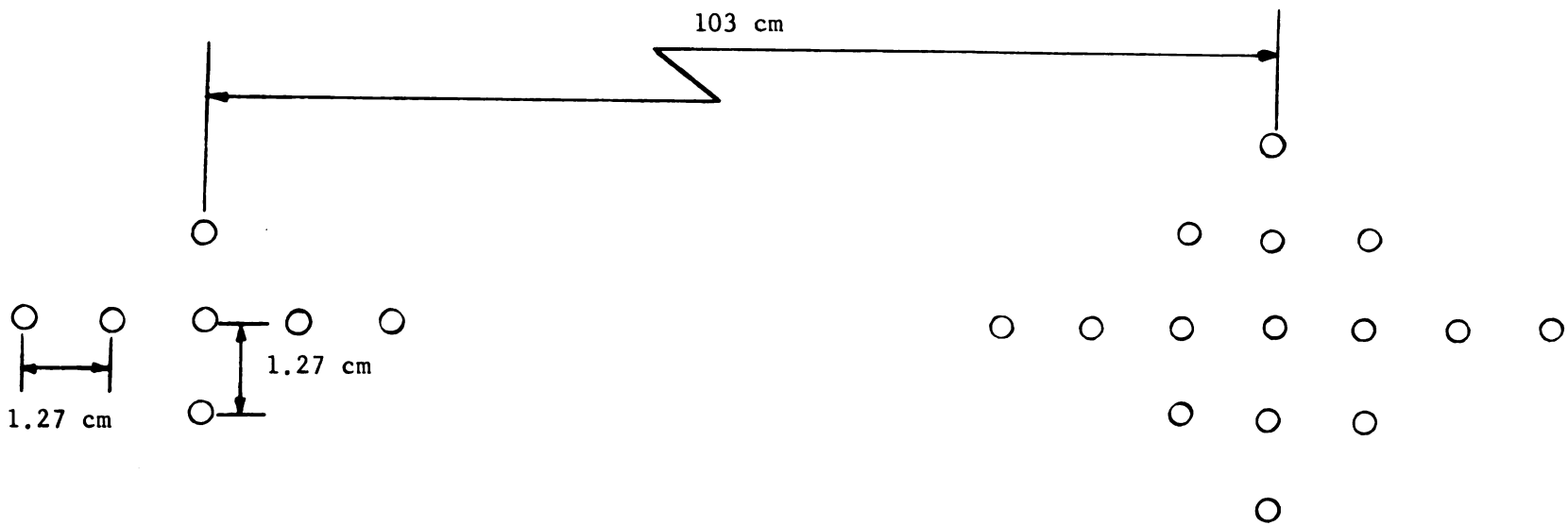

a) Upstream or Inflow Set

b) Downstream or Outflow Set

Fig. 3-6 Electrode Groups

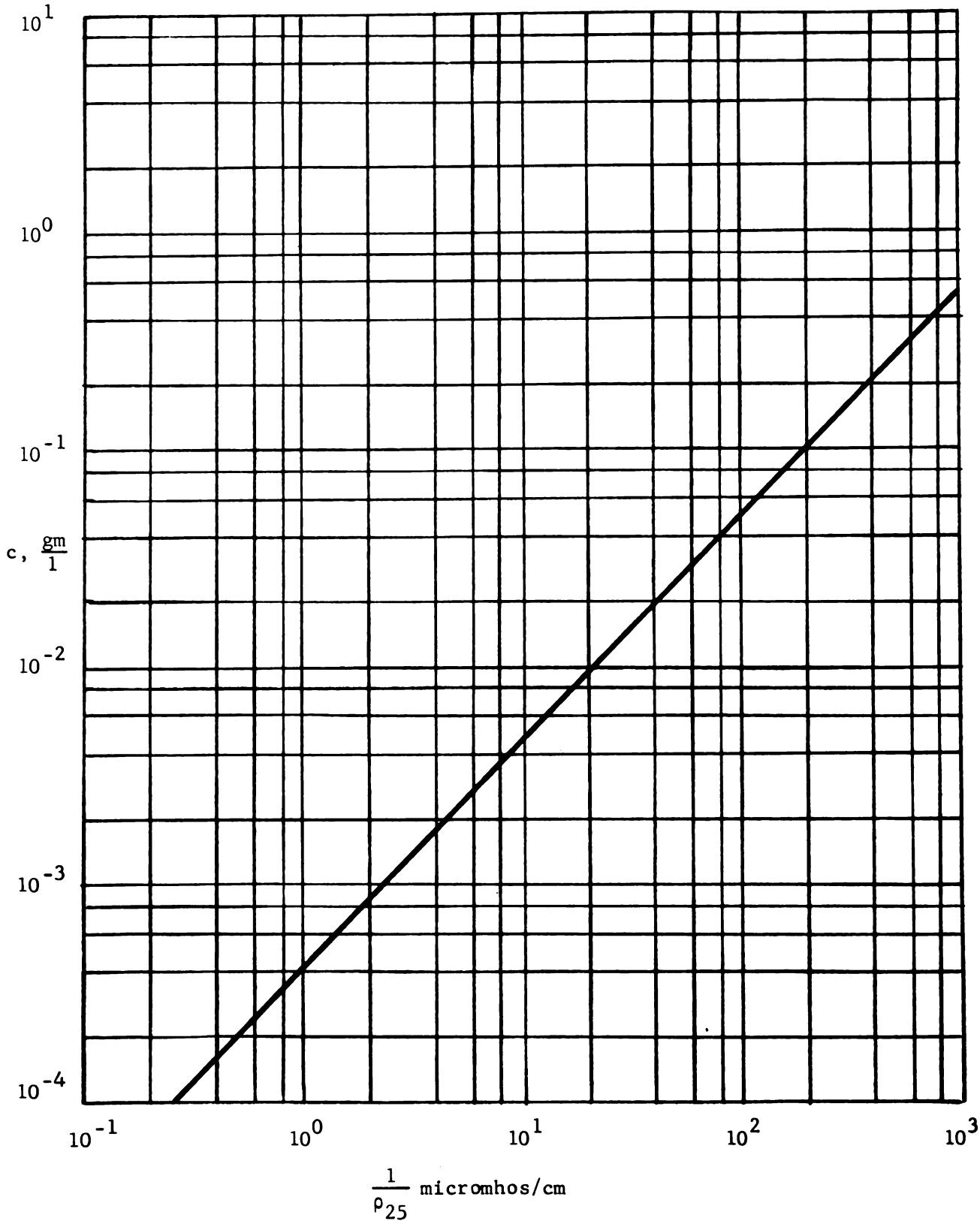

Fig. 4-1 Concentration of NaCl in water is a function of specific conductance T = 25°C

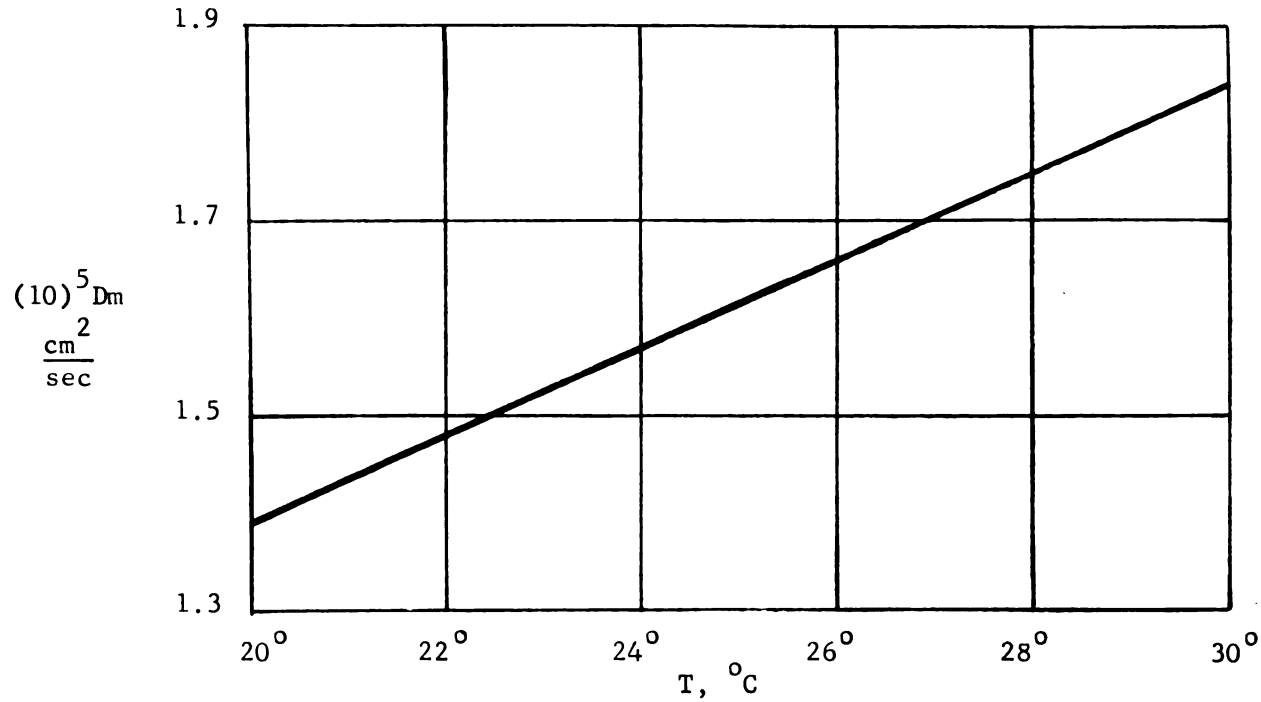

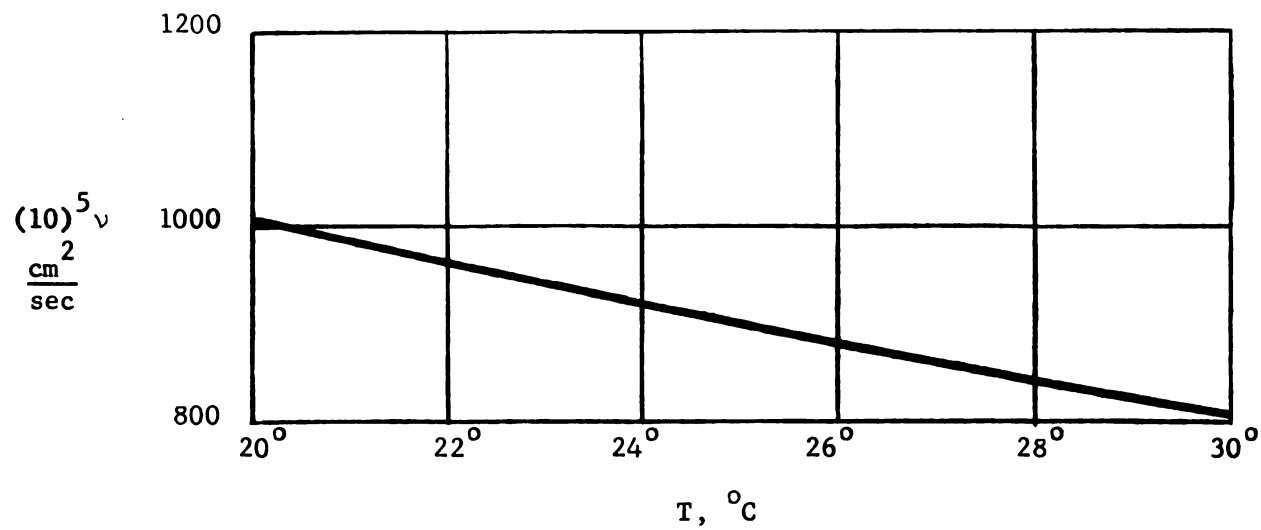

Fig. 4-2 Molecular Diffusivity and Kinematic Viscosity

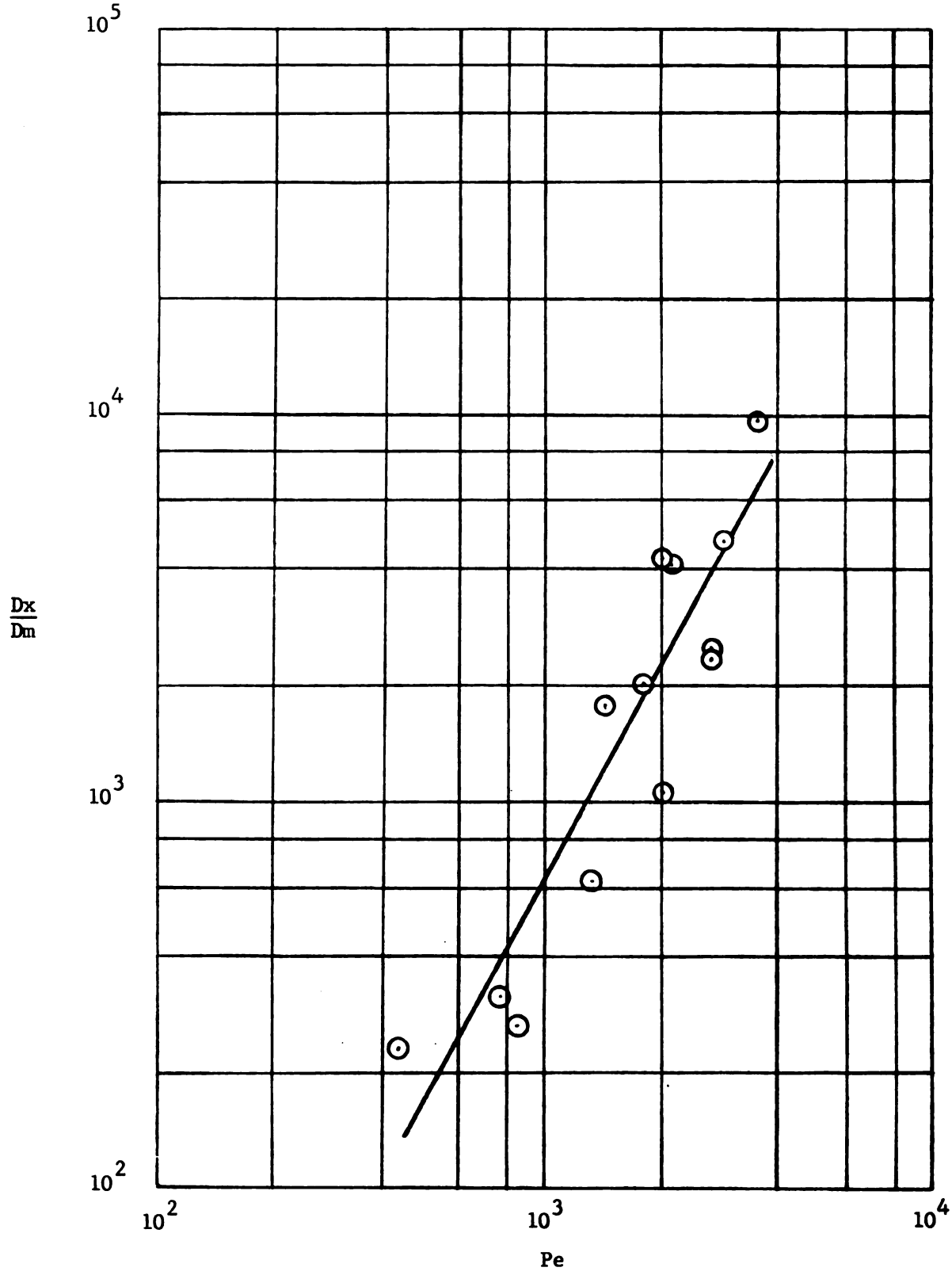

Fig. 4-3a Bed 1 $\frac{Dx}{Dm}$ versus Pe

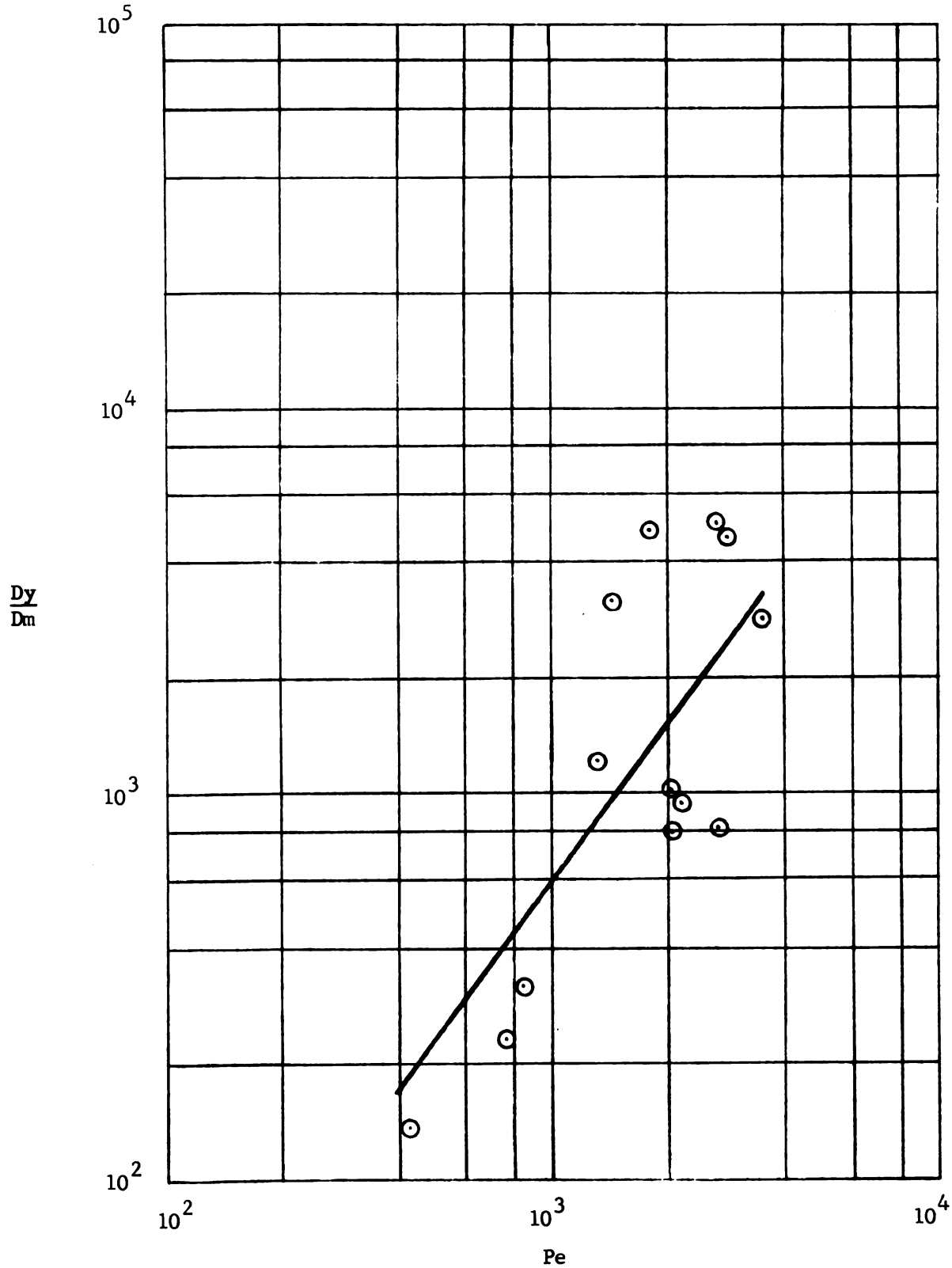

Fig. 4-3b Bed 1 $\frac{Dy}{Dm}$ versus Pe

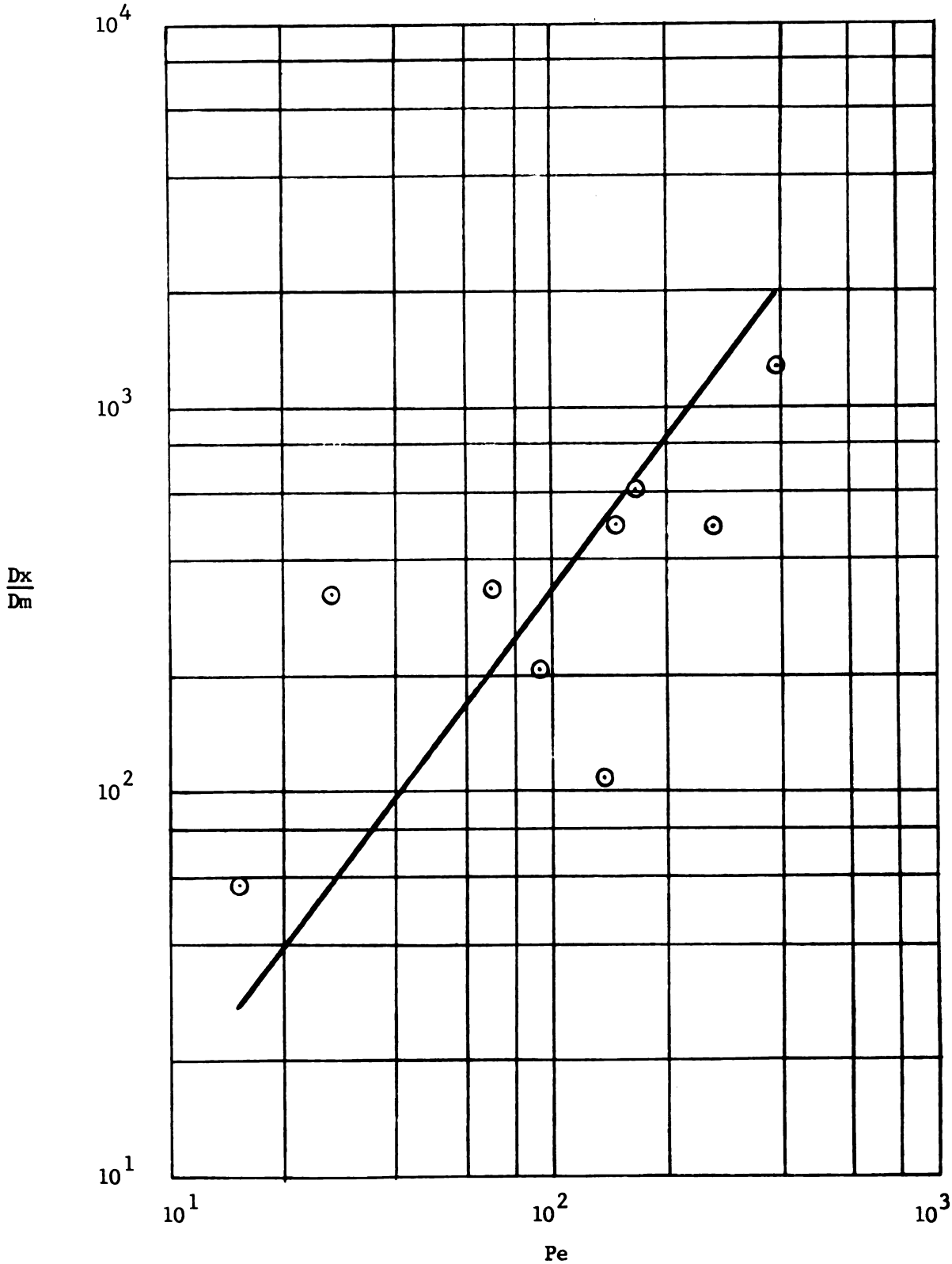

Fig. 4-4a Bed 2 $\frac{Dx}{Dm}$ versus Pe

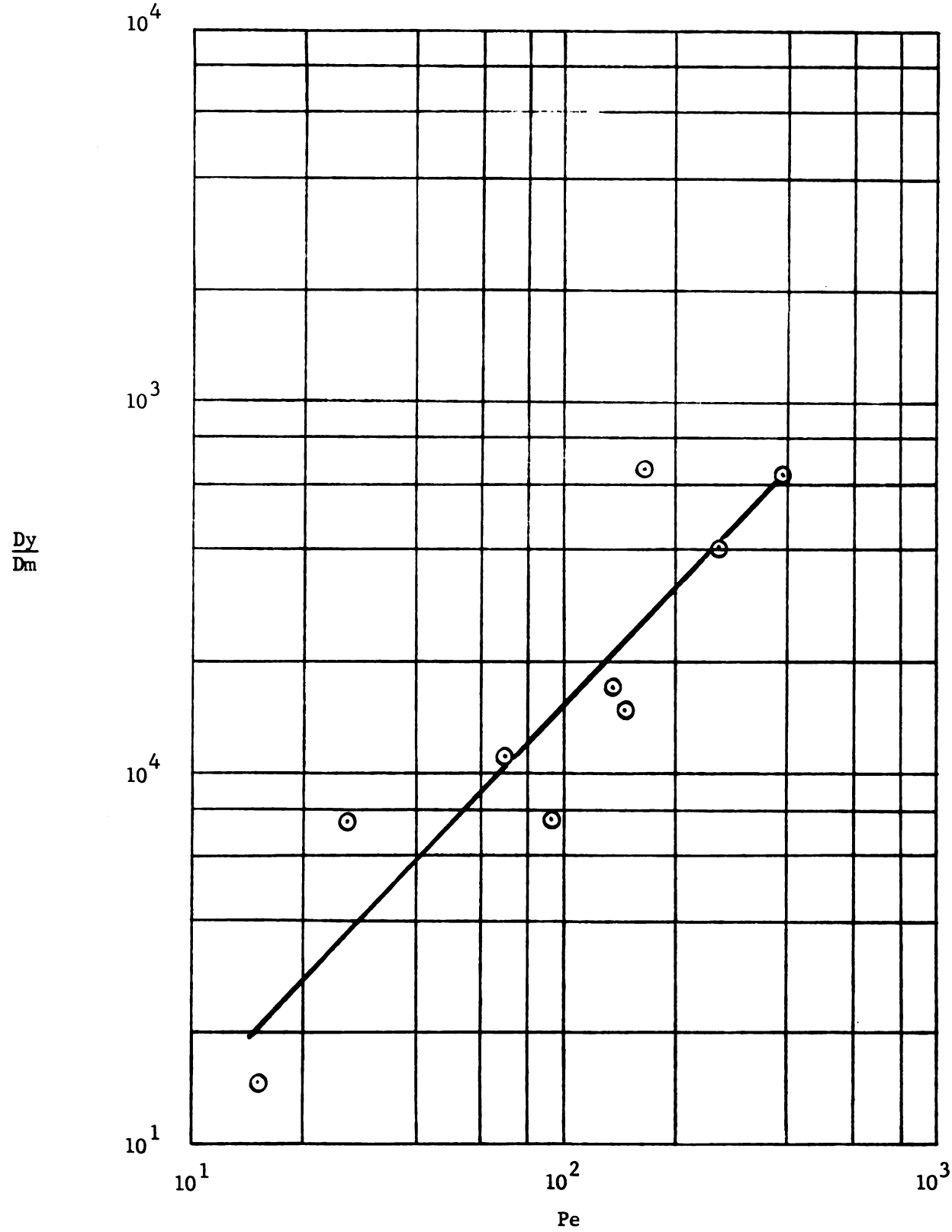

Fig. 4-4b Bed 2 $\frac{Dy}{Dm}$ versus Pe

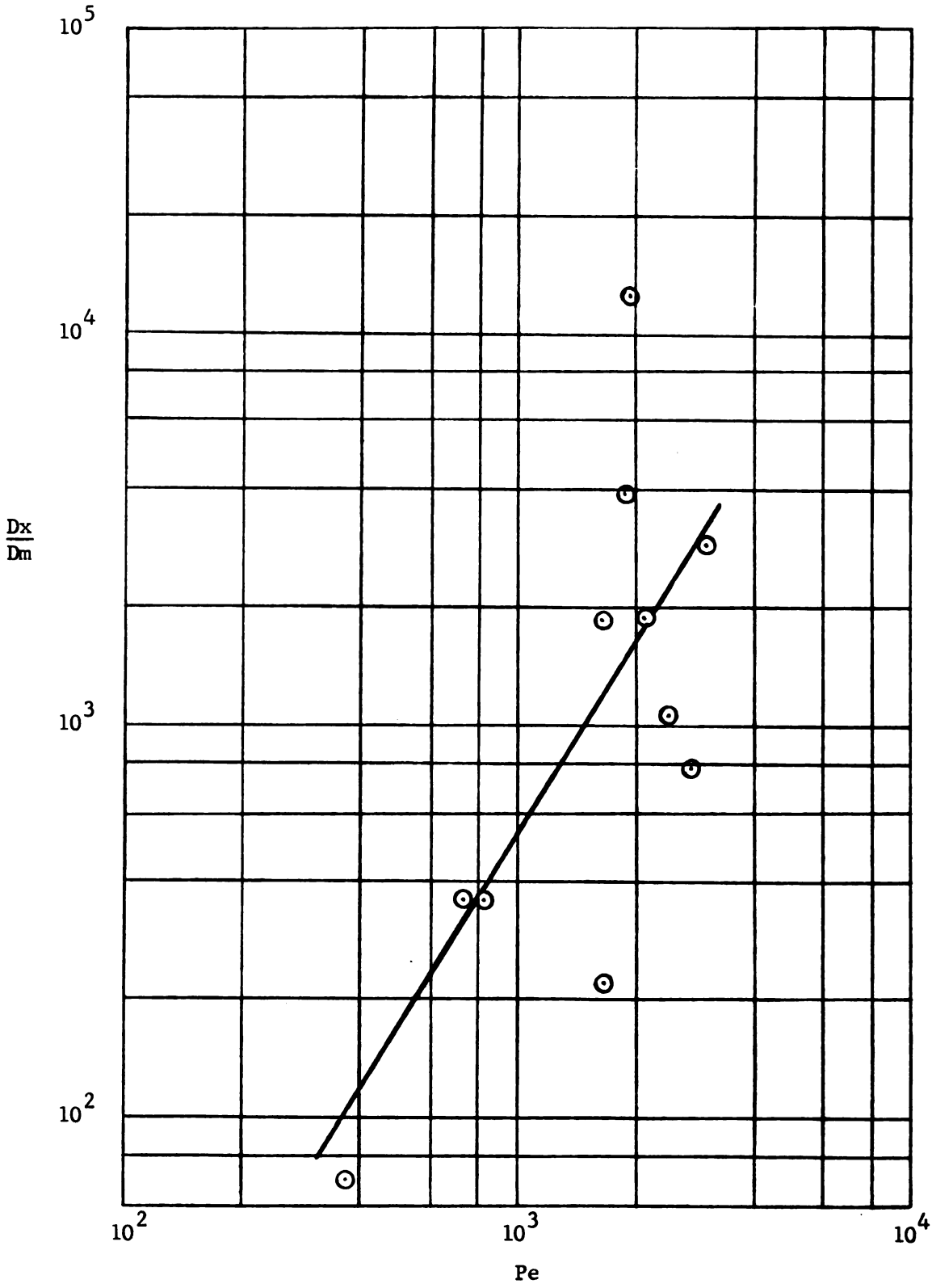

Fig. 4-5a Bed 3 $\frac{Dx}{Dm}$ versus Pe

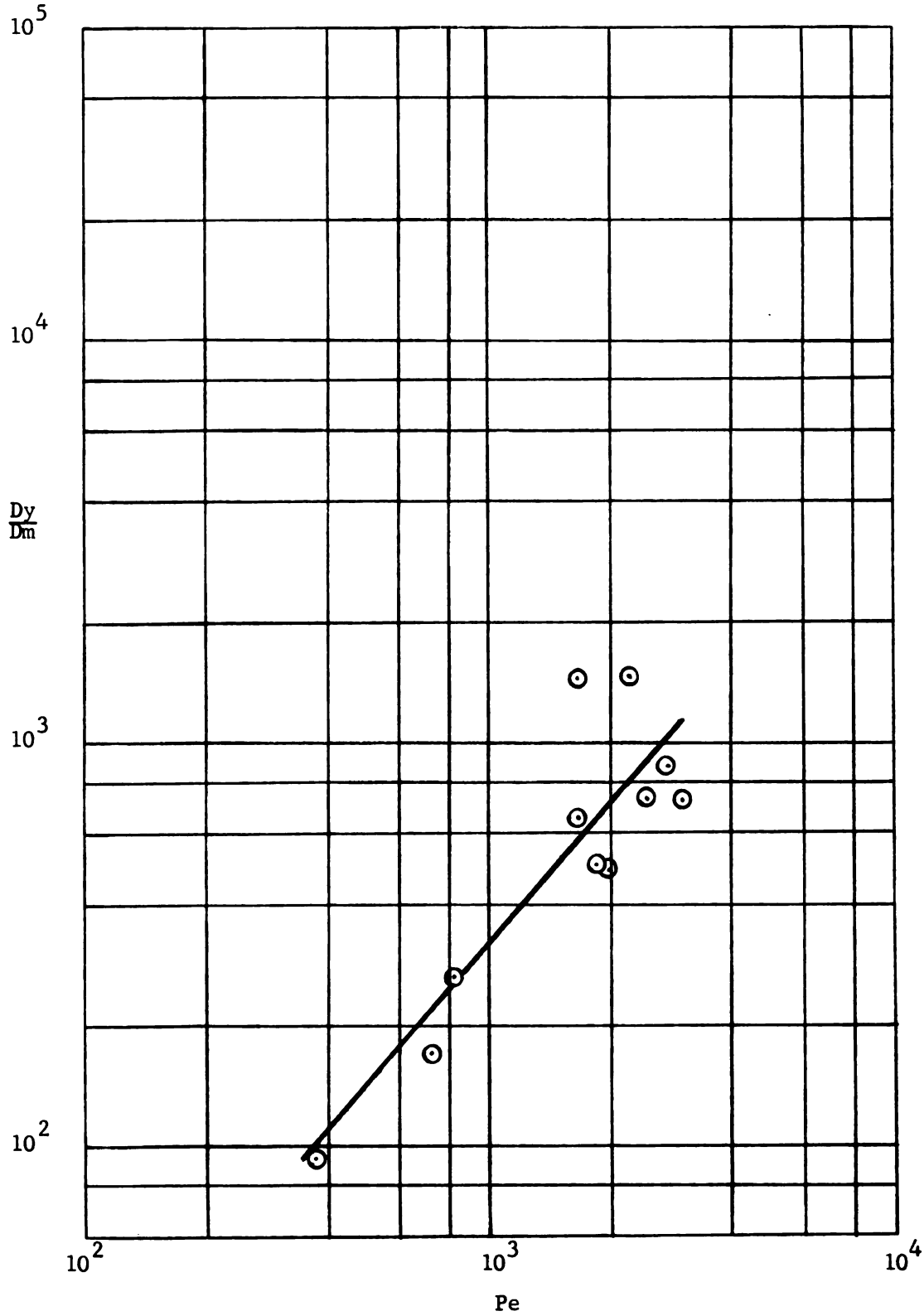

Fig. 4-5b Bed 3 $\frac{Dy}{Dm}$ versus Pe

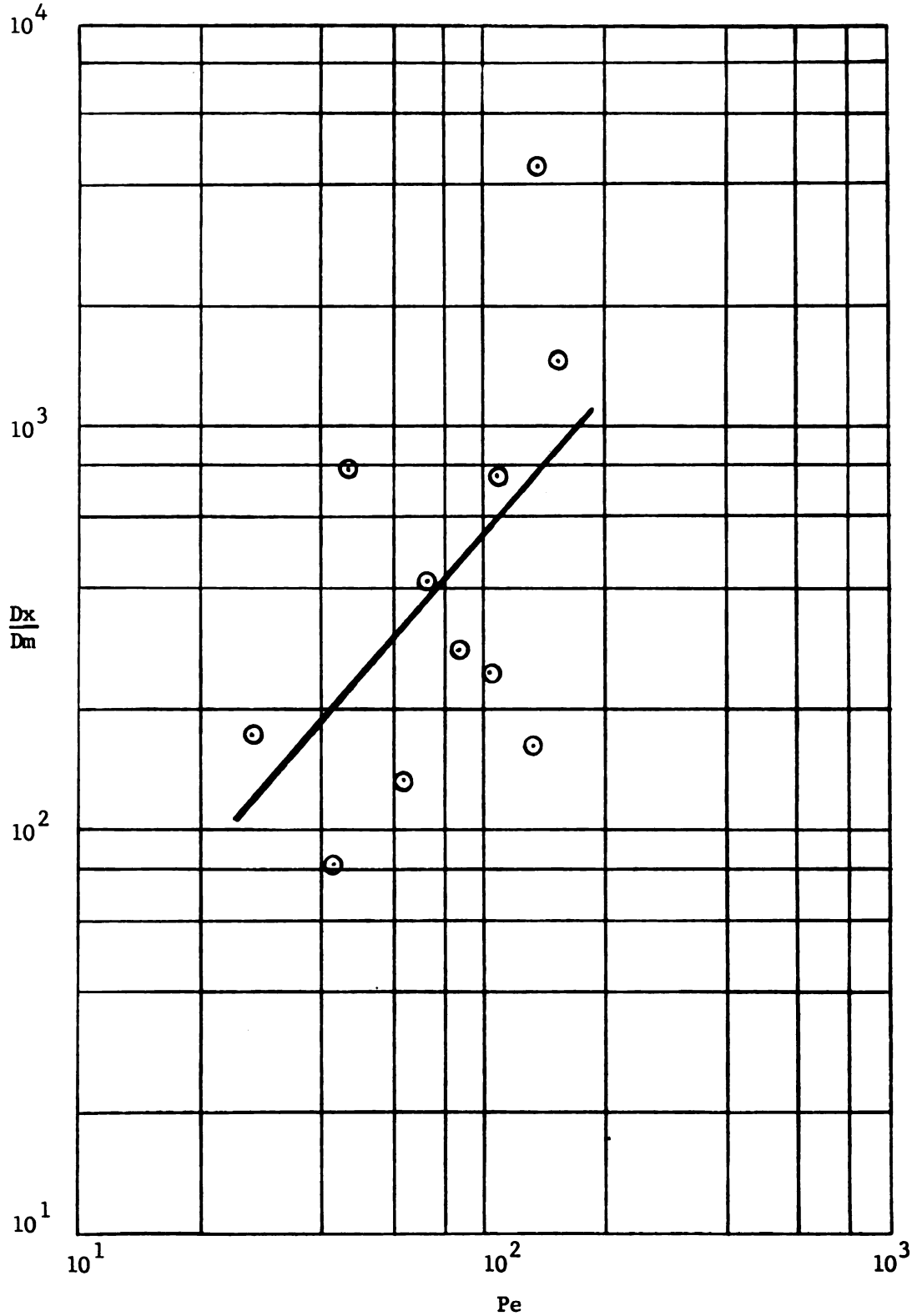

Fig. 4-6a Bed 4 $\frac{Dx}{Dm}$ versus Pe

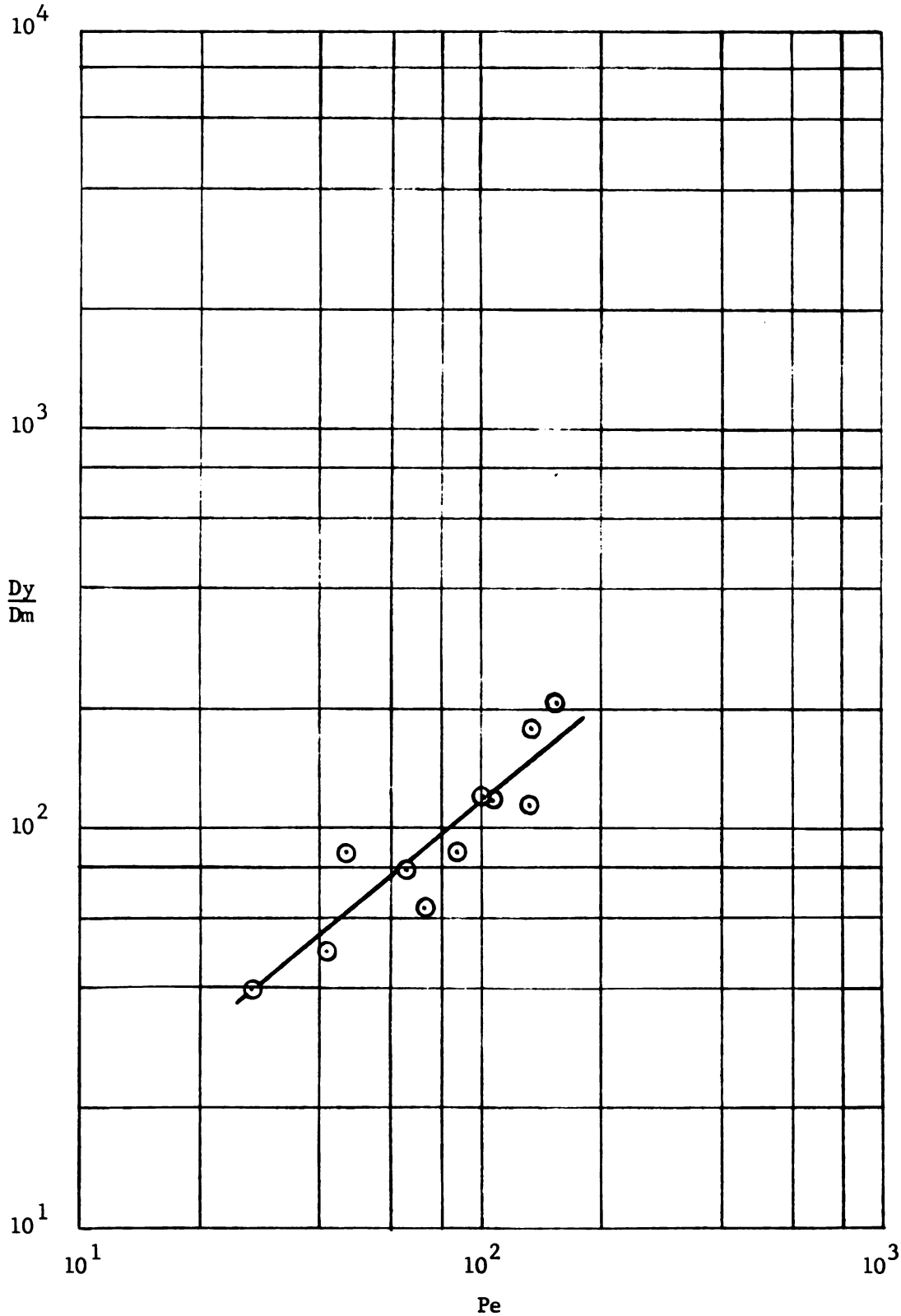

Fig. 4-6b Bed 4 $\frac{Dy}{Dm}$ versus Pe

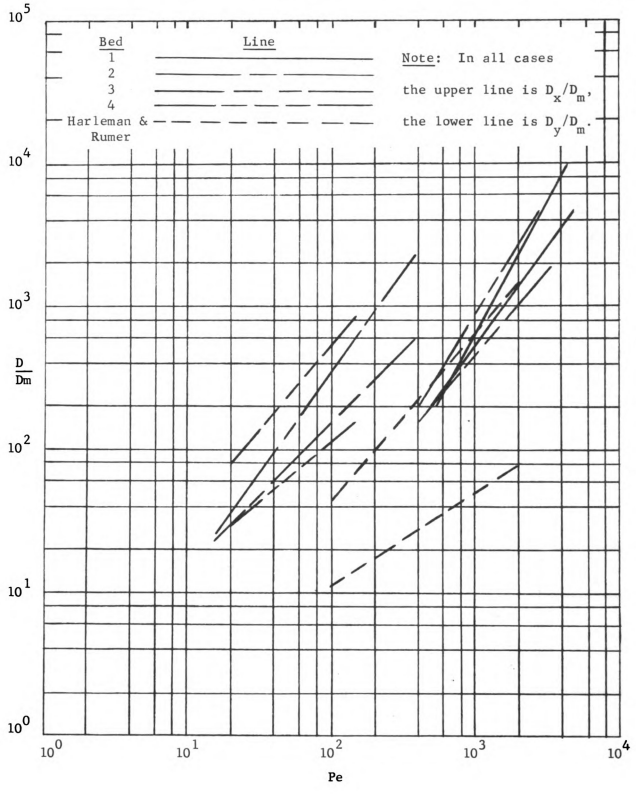

Fig. 4-7 Composite Plot of Data

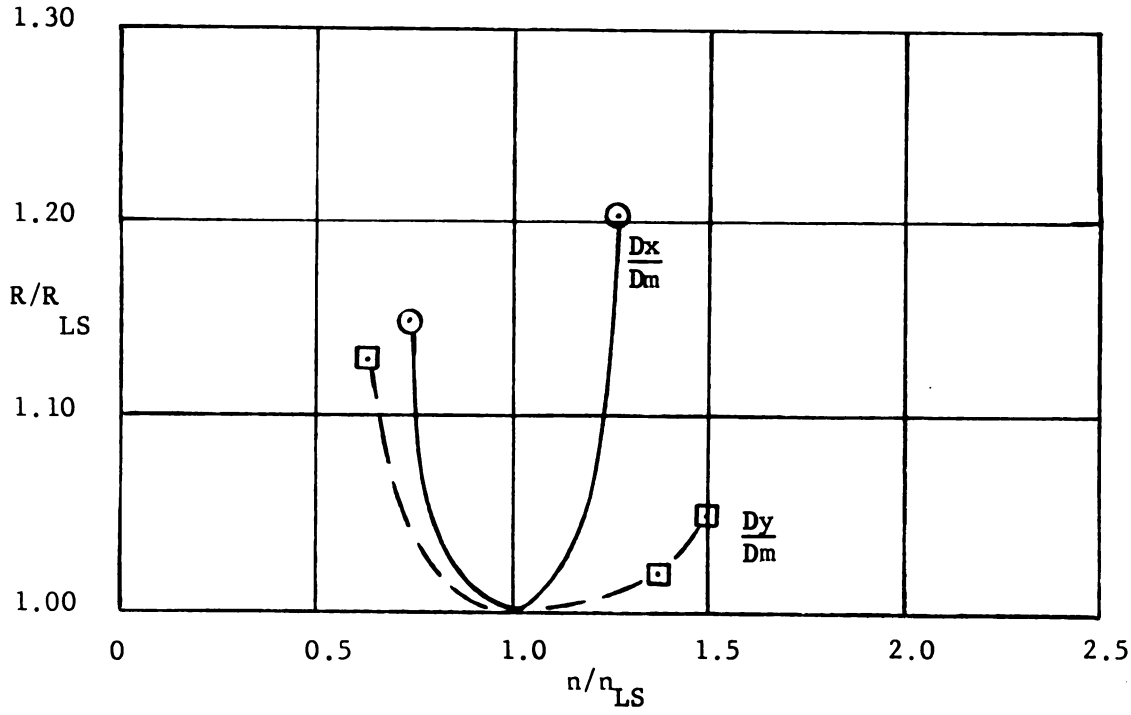

Fig. A-1 Bed 1 R/R_{LS} versus n/n_{LS}

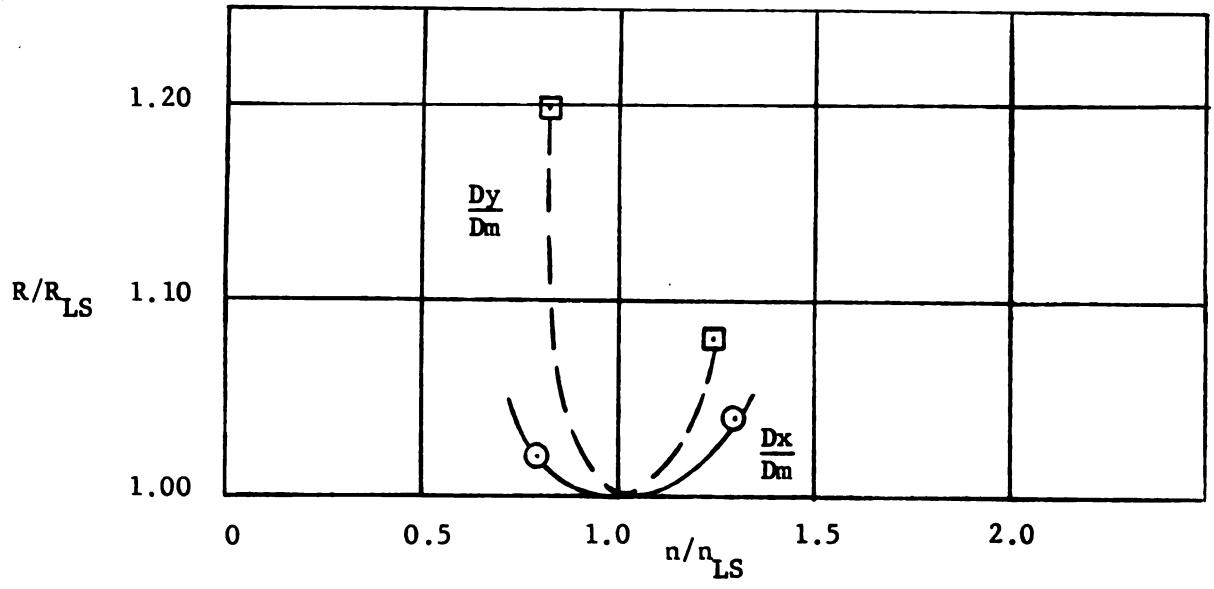

Fig. A-2 Bed 3 R/R_{LS} versus n/n_{LS}

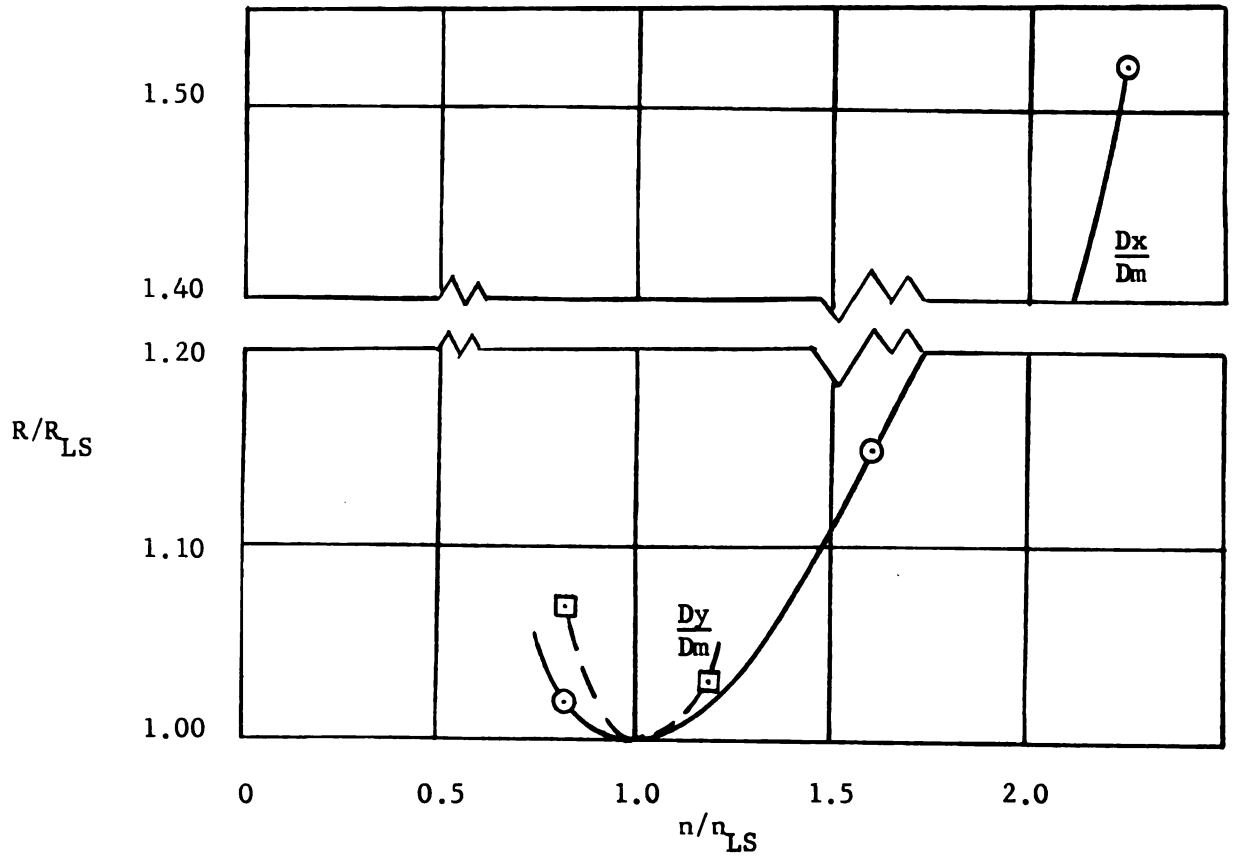

Fig. A-3 Bed 2 R/R_{LS} versus n/n_{LS}

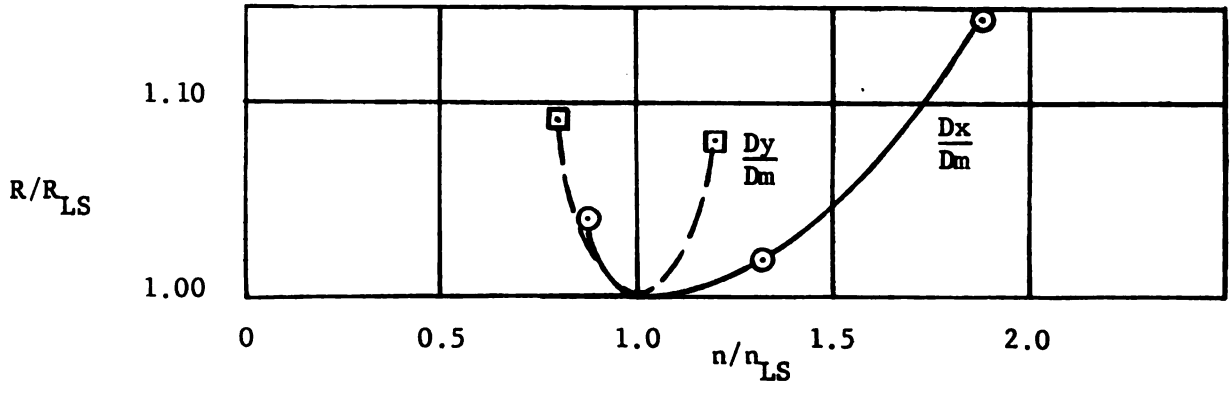

Fig. A-4 Bed 4 R/R_{LS} versus n/n_{LS}

BIBLIOGRAPHY

Aris, R., Vectors, Tensors, and the Basic Equation of Fluid Mechanics, Prentice-Hall, Inc., Englewood Cliffs, N. J., 1962.

Bear, J., "On the tensor form of dispersion in porous media," Journal of Geophysical Research, Vol. 66, No. 10, 1961.

Bear, J., and Todd, D. K., "The transition zone between fresh and salt waters in coastal aquifers," Contribution No. 29, Water Resources Center, University of California, 1960.

Bell, J. R. and Grosberg, P., "Diffusion through porous materials," Nature, Vol. 198, No. 4769, March, 1961.

Benson, M. A., "Spurious correlations in hydraulics and hydrology," Journal of the Hydraulics Division, Proceedings ASCE, Vol. 91, No. HY 4, July, 1965.

Carrier, G. F., "The mixing of ground water and sea water in permeable subsoils," Journal of Fluid Mechanics, Vol. 4, No. 5, 1958.

Collins, R. E., Flow of Fluids Through Porous Materials, Reinhold Publishing Corporation, New York, 1961.

Harleman, D. R. F., Mehlhorn, P. F., and Rumer, R. R. Jr., "Dispersion permeability correlation in porous media," Journal of the Hydraulics Division, Proceedings ASCE, Vol. 89, No. HY2, May, 1963.

Harleman, D. R. F., and Rumer, R. R. Jr., "The dynamics of salt-water intrusion in porous media," Report No. 55, Hydromechanics Laboratory, Massachusetts Institute of Technology, August, 1962.

Harr, M. E., Groundwater and Seepage, McGraw-Hill Book Co., Inc. New York, 1962.

Hawley, M. C., "Solute dispersion in liquid-solid chromatographic columns," Thesis for the degree of Ph.D., Michigan State University, 1964.

Henry, H. R., "Salt water intrusion into fresh water aquifers," Journal of Geophysical Research, Vol. 64, No. 11, 1959.

Henry, H. R., "Salt Intrusion into Coastal Aquifers," Commission of subteranean water, International Association for Scientific Hydrology, Publication No. 52, 1960.

B I B L I O G R A P H Y (continued)

Hildebrand, F. B., Advanced Calculus for Engineers, Prentice-Hall, Inc., New York, 1949.

De Josselin de Jong, G., "Longitudinal and transverse diffusion in granular deposits," Transactions of the American Geophysical Union, Vo. 39, 1958.

De Josselin de Jong, G., "Vortex theory for multiple phase flow through porous media," Contribution No. 23, Water Resources Center, University of California, 1959.

Kohout, F. A., "Cyclic flow of fresh water in the Biscayne aquifer of northeastern Florida," Journal of Geophysical Research, Vol. 65, 1960.

Lin, K. M., "Transient twophase flow through porous media," Thesis for degree of Ph.D., Michigan State University, 1964.

Muskat, M., Flow of Homogeneous Fluids through Porous Media, J. W. Edwards, Inc., Ann Arbor, Michigan, 1946.

Ogata, A., "Transverse diffusion in saturated isotropic granular media," Professional Paper No. 411-B, U. S. Geological Survey, 1961.

Ogata, A. and Banks, R. B., "A solution of the differential equation of longitudinal dispersion in porous media," Professional Paper No. 411-A, U. S. Geological Survey, 1961.

Polubarinova-Kochina, P. Ya., Theory of Groundwater Movement, Translated from Russian by J. M. R. De Wiest, Princeton University Press, 1962.

von Rosenberg, D. U., "Mechanics of steady state single-phase fluid displacement from porous media, Journal, AIChE, Vol. 2, No. 1, 1956.

Saffman, P. G., "A Theory of dispersion in porous media," Journal of Fluid Mechanics, Vol. 6, 1959.

Saffman, P. G., "Dispersion due to Molecular diffusion and macroscopic mixing in flow through a network of capillaries," Journal of Fluid Mechanics, Vo.. 7, 1960.

Scheidegger, A. E., "Statistical hydrodynamics in porous media," Journal of Applied Physics, Vol. 25, No. 8, 1954.

Scheidegger, A. E., The Physics of Flow Through Porous Media, The Mac-Millan Company, New York, 1960.

Scheidegger, A. E., "General theory of dispersion in porous media," Journal of Geophysical Research, Vol. 66, No. 4, 1961.

B I B L I O G R A P H Y (continued)

Simpson, E. S., "Transverse dispersion in liquid flow through porous media," Professional Paper No. 411-C, U. S. Geological Survey, 1962.

Taylor, G. I., "Dispersion of soluble matter in solvent flowing slowly through a tube," Proceedings, Royal Society of London, Vol. 219, Series A, 1953.

Todd, D. K., Groundwater Hydrology, John Wiley & Sons, New York, 1959.

Wentworth, C. K., "Growth of the Gyben-Herzberg transition zone under a rinsing hypothesis," Transactions American Geophysical Union, Vol. 29, No. 1, 1948.